Aging Cell

miR-17, miR-19b, miR-20a and miR-106a are down-regulated in human aging

Journal:	*Aging Cell*
Manuscript ID:	ACE-09-0262.R1
Manuscript Type:	Short Take
Date Submitted by the Author:	27-Nov-2009
Complete List of Authors:	Hackl, Matthias; University of Natural Resources and Applied Life Sciences Vienna, Dept. of Biotechnology Brunner, Stefan; Institute for Biomedical Aging Research, Department of Immunology Fortschegger, Klaus; University of Natural Resources and Applied Life Sciences Vienna, Dept. of Biotechnology Schreiner, Carina; University of Natural Resources and Applied Life Sciences Vienna, Dept. of Biotechnology Micutkova, Lucia; Institute for Biomedical Aging Research, Dept. of Molecular and Cell Biology Mück, Christoph; Institute for Biomedical Aging Research, Dept. of Molecular and Cell Biology Laschober, Gerhard; Institute for Biomedical Aging Research, Extracellular Matrix Research Lepperdinger, Günter; Institute for Biomedical Aging Research, Extracellular Matrix Research Sampson, Natalie; Institute for Biomedical Aging Research, Dept. of Endocrinology Berger, Peter; Institute for Biomedical Aging Research, Dept. of Endocrinology Herndler-Brandstetter, Dietmar; Institute for Biomedical Aging Research, Immunology Wieser, Matthias; University of Natural Resources and Applied Life Sciences Vienna, Dept. of Biotechnology; University of Natural Resources and Applied Life Sciences, Institute of Applied Microbiology Kühnel, Harald; University of Veterinary Medicine Vienna, Department of Natural Sciences Strasser, Alois; University of Veterinary Medicine Vienna, Department of Natural Sciences Grillari, Johannes; University of Natural Resources and Applied

Keywords:	molecular biology of aging, Replicative Senescence, chronological aging, human, miroRNA, miR-17-92, p21 CDKN1A

miR-17, miR-19b, miR-20a and miR-106a are down-regulated in human aging

Running title: miRNAs in replicative and organismal aging

Matthias Hackl[1#], Stefan Brunner[2#], Klaus Fortschegger[1§], Carina Schreiner[1], Lucia Micutkova[3], Christoph Mück[3], Gerhard T. Laschober[4], Günter Lepperdinger[4], Natalie Sampson[5], Peter Berger[5], Dietmar Herndler-Brandstätter[2], Matthias Wieser[1], Harald Kühnel[6], Alois Strasser[6], Mark Rinnerthaler[7], Michael Breitenbach[7], Michael Mildner[8], Leopold Eckhart[8], Erwin Tschachler[8], Andrea Trost[9], Johann W. Bauer[9], Christine Papak[10], Zlatko Trajanoski[10], Marcel Scheideler[10], Regina Grillari-Voglauer[1], Beatrix Grubeck-Loebenstein[2], Pidder Jansen-Dürr[3], and Johannes Grillari[1*]

[1]Aging and Immortalization Research, Department of Biotechnology, University of Natural Resources and Applied Life Sciences, Vienna, Austria, Muthgasse 18, A-1190 Vienna
[2]Department of Immunology, Institute for Biomedical Aging Research , Austrian Academy of Sciences, Rennweg 10, 6020 Innsbruck, Austria (IBA)
[3]Department of Molecular and Cell Biology, (IBA)
[4]Department of Extracellular Matrix Research, (IBA)
[5]Department of Endocrinology, (IBA)
[6] Institute of Physiology, Department of Natural Sciences, University of Veterinary Medicine Vienna, Veterinärplatz 1, A-1210 Wien, Austria
[7]Department of Genetics, University of Salzburg, Heilbrunnerstraße 34, 5020 Salzburg, Austria
[8]Department of Dermatology, Medical University of Vienna, A-1090 Vienna, Austria
[9]Department of Dermatology, SALK and Paracelsus Medical University, Salzburg, Austria
[10]Institute for Genomics and Bioinformatics and Christian Doppler Laboratory for Genomics and Bioinformatics, Graz University of Technology, Petersgasse 14, 8010 Graz, Austria

Keywords: aging, senescence, miRNA microarray, miR-17-92 cluster, p21 (CDKN1A), miR-17, miR-19b, miR-20a, miR-106a

# authors contributed equally to this work
*to whom correspondence should be addressed:
Aging and Immortalization Research, Department of Biotechnology, University of Natural Resources and Applied Life Sciences, Vienna, Austria
Muthgasse 18, A-1190 Vienna, Tel: +43-1-47654 6231, FAX: + 43-1-3697615, email: johannes.grillari@boku.ac.at
§ present address: Children's Cancer Research Institute, Zimmermannplatz 10, 1090 Vienna

Summary

Aging is a multifactorial process where deterioration of body functions is driven by stochastic damage while counteracted by distinct genetically encoded repair systems. In order to better understand the genetic component of aging, many studies have addressed the gene and protein expression profiles of various aging model systems engaging different organisms from yeast to human. The recently identified small non-coding miRNAs are potent post-transcriptional regulators that can modify the expression of up to several hundred target genes per single miRNA, similar to transcription factors. Increasing evidence shows that miRNAs contribute to the regulation of most if not all important physiological processes, including aging. However, so far the contribution of miRNAs to age-related and senescence-related changes in gene expression remains elusive. To address this question, we have selected 4 replicative cell aging models including endothelial cells, replicated $CD8^+$ T cells, renal proximal tubular epithelial cells, and skin fibroblasts. Further included were three organismal aging models including foreskin, mesenchymal stem cells and $CD8^+$ T cell populations from old and young donors. Using LNA-based miRNA microarrays we identified four commonly regulated miRNAs, miR-17 down-regulated in all 7, miR-19b and miR-20a, down-regulated in 6 models and miR-106a down-regulated in 5 models. Decrease in these miRNAs correlated with increased transcript levels of some established target genes, especially the cdk inhibitor p21/CDKN1A. These results establish miRNAs as novel markers of cell aging in humans.

Short take

Continuous stochastic damage contributes to the gradual attenuation of physiologic functions, which are partially alleviated by genetically encoded repair systems (Kirkwood, 2008). Genetic determinants which have a direct impact on these biological processes can be characterized by either studying model organisms that are amenable to genetic manipulations (Lepperdinger *et al.*, 2008), or by applying functional genomic methods. Both strategies have helped to identify genes and proteins which potentially modulate the aging process. Proteins identified in various studies have been compiled in a database only recently (de Magalhaes *et al.*, 2009). Yet, hardly any study has so far addressed the role of miRNAs during aging (Bates *et al.*, 2009; Grillari & Grillari-Voglauer, in press).

MiRNAs are a class of small non-coding silencing RNAs of approximately 22 nucleotides in length (Ghildiyal & Zamore, 2009). They confer specificity to the RNA induced silencing complex that either degrades or translationally represses target mRNAs (Bhattacharyya *et al.*, 2006; Carthew & Sontheimer, 2009). Since the recognition of target mRNAs mainly depends on the small seed region within the mature miRNA, a single miRNA potentially regulates up to several hundred mRNA targets, thus orchestrating a large variety of cellular processes (Lim *et al.*, 2005; Stefani & Slack, 2008).

Here, we have set out to systematically compare miRNA transcription profiles in old versus young human cells. Employed were *in vitro* replicative senescence of endothelial cells (Chang *et al.*, 2005; Hampel *et al.*, 2006), renal proximal tubular epithelial cells (Wieser *et al.*, 2008), skin fibroblasts (Hutter *et al.*, 2002; Stockl *et al.*, 2006) as well as an intra-individual comparison of *in vivo* replicatively exhausted $CD8^+$ T cells (Saurwein-Teissl *et al.*, 2002; Effros *et al.*, 2005). Furthermore, we used bone-derived mesenchymal stem cells (Fehrer *et al.*, 2007; Laschober *et al.*, 2009), foreskin (Oender *et al.*, 2008), as well as $CD8^+$ $CD28^+$ T cells from young versus old donors (Lazuardi *et al.*, 2009). Detailed characterization of these models as well as an overview over biological and technical replicates and experimental design is presented in the supplements (Fig. S1 and Fig. S2A). Experiments were approved by the local ethical committees and written informed consent is available from all donors.

LNA-miRNA microarrays were spotted (Castoldi *et al.*, 2006) using Sanger miRBase v9.2 (Griffiths-Jones *et al.*, 2008) probe sets consisting of 559 human, 170 mouse

and 77 not yet annotated (miRPlus sequences, Exiqon Inc.) miRNA probes. Microarray design, a comprehensive set of related protocols as well as raw and normalized intensity data have been submitted to Array Express Database compliant to MIAME standards (Brazma *et al.*, 2001; Brazma, 2009). For Array Express accession numbers and detailed materials and methods see supplementary information and Fig. S2A.

Depending on the experimental system, statistical analysis identified 10-20% of the miRNAs as regulated, while the majority remained unchanged during aging (Table S1). Applying hierarchical clustering of all regulated miRNAs, members of the miR-17-92 cluster and paralogous clusters stood out as being commonly down-regulated (Fig. S3).

Using linear models and moderated T-statistics (Smyth, 2004) in combination with false-discovery-rate (FDR) adjustment according to Benjamini-Hochberg, we calculated differential expression of miRNAs (FDR-adjusted p-value < 0.05) for each of the 7 model systems independently (available as tab-delimited sheet in Table S2). Intersections of these lists of regulated miRNAs were then analyzed for the replicative aging models and the ex vivo models which resulted in 5 miRNAs with common expression changes in replicative aging and 34 miRNAs that changed expression during organismal aging (Fig 1A). Interestingly, both replicative and organismal aging, share a common set of 4 miRNAs ("public miRNAs") that belong to the miR-17-92 cluster or its paralogous cluster miR-106a-363 and are down-regulated in both conditions (Fig. 1B). Fig. 1B shows that microarray analysis identified miR-17 as significantly down-regulated in all 7 model systems, while miR-19b, and miR-20a are down-regulated in 6 and miR-106a in 5 out of the 7 model systems. Interestingly, 3 out of these four miRNAs also share the same seed sequence (Fig. 1C) indicating a cooperative relief of translational inhibition of a common and important set of target genes. Although low transcription levels of mature miR-17 have been found in S-phase cells compared to G0/G1 and G2/M phase HeLa cells (Cloonan *et al.*, 2008), our result is not a mere growth arrest phenomenon, since miR-17 and miR-19b are not regulated in young replicating versus quiescent endothelial cells (data not shown).

Using quantitative PCR we confirmed the down-regulation of miR-17, miR-19b, miR-20a and miR-106a (Fig. 2A) but observed a greater dynamic range in fold changes

ranging up to a 6-fold down-regulation, thus indicating an even stronger decrease in the transcription of all four miRNAs with age.

Down-regulation of members of the miR-17-92 cluster has been reported recently in aging related conditions like in stress induced senescence (G. Li *et al.*, 2009), after p53 induction (Brosh *et al.*, 2008) as well as after low level irradiation (Maes, An, Sarojini, Wu *et al.*, 2008) of human fibroblasts.

However, other reports on differential expression of miRNAs in replicative senescence of fibroblasts (Brosh *et al.*, 2008; Lal *et al.*, 2008; Bhaumik *et al.*, 2009; Maes *et al.*, 2009), in senescence of mesenchymal stem cells (Wagner *et al.*, 2008), of human and mouse brain tissue (Lukiw, 2007; N. Li *et al.*, 2009) as well as of murine liver (Maes, An, Sarojini and Wang, 2008) and lung (Williams *et al.*, 2007; Izzotti *et al.*, 2009) do not not explicitly report regulation of miR-17-92 miRNAs. This might either be due to the fact that in some studies only up-regulated miRNAs have been reported or to the strategy, that only at least 2-fold changed miRNAs were considered.

Since the ability of array platforms to detect fold changes down to 1.3 fold (Wurmbach *et al.*, 2003) and since LNA based microarray methodology is considered to be one of the most sensitive and reliable at the moment (Willenbrock *et al.*, 2009), we included miR-17-92 cluster members that are significantly regulated even at levels below 2-fold, even more so, since array results also are reported to have the tendency to under-estimate the ratios (Wurmbach *et al.*, 2003).

Interestingly, among the published targets of the miR-17-92 cluster is p21/CDKN1A mRNA (Ivanovska *et al.*, 2008; Inomata *et al.*, 2009). Indeed, p21/CDKN1A mRNA levels are negatively correlated in all model systems (Fig. 2B), although the ratio in old versus young T-cells does not reach significance.

These data indicate that the miR-17-92 cluster, which is known to contribute to transcriptional regulation in cell cycle control and tumorigenesis (He *et al.*, 2005), also contributes to transcriptional regulation in senescence and aging, consistent with the known interdependence between senescence and tumorigenesis (Campisi, 2003; Rodier *et al.*, 2007).

Among others, E2F transcriptionally activates (Woods *et al.*, 2007) and p53 represses the miR-17-92 cluster (Yan *et al.*, 2009). Thus decreased miR-17-92 levels are consistent with the notion that, E2F family members decrease (Dimri *et al.*,

1994), while p53 activity increases in senescence (Atadja *et al.*, 1995; Kulju & Lehman, 1995).

Downstream of miR-17-92 are 19 experimentally confirmed mRNA targets besides p21. Many of them are involved in tumorigenesis and cell cycle control (Tab. S3). Indeed, miR-17-92 suppression induces growth arrest in anaplastic thyroid cancer cell models (Takakura *et al.*, 2008). Furthermore, an increase in the level of miR-17-92 is associated with a decrease of ROS and DNA damage in RB mutated tumor cells (Ebi *et al.*, 2009). It will be exciting to test in an experimental system whether a decrease of miR-17-92, as detected in our models of aging, conversely results in more ROS and DNA damage, both well accepted driving forces of age-related functional decline.

In summary, our results implicate specific changes of miRNA abundance and activity in a broad range of human aging models and suggest the use of miR-17 and 19b as novel biomarkers of cellular aging.

Acknowledgements

This work was supported by NRN grant S93 of the Austrian Science Fund, the GEN-AU Project 820982 „Non-coding RNAs" to JG and MS as well as grants by the Herzfelder'sche Familienstiftung and CE.R.I.E.S to JG. DHB is supported by a European FLARE fellowship funded by the Austrian Federal Ministry of Science and Research (BMWF).

Author contributions

KF, CS and MH designed experiments and performed array analysis. MW, JG and RGV designed experiments for RPTECs; HK, AS, NS, PB and RGV designed experiments for HDFs; LM, CM and PJD designed experiments and provided HUVECs; SB, DHB and BGL designed experiments for T cell model; MR, MB, LE, MM, and ET designed experiments for foreskin; AT and JWB provided foreskin; GTL and GL designed experiments for MSCs; CP, MS, ZT planned and spotted LNA based miRNA arrays; MH, SB and JG planned the study, interpreted the data, and wrote the manuscript.

References

Atadja P, Wong H, Garkavtsev I, Veillette C, Riabowol K (1995) Increased activity of p53 in senescing fibroblasts. *Proc Natl Acad Sci U S A* **92,** 8348-8352.

Bates DJ, Liang R, Li N, Wang E (2009) The impact of noncoding RNA on the biochemical and molecular mechanisms of aging. *Biochim Biophys Acta*.

Bhattacharyya SN, Habermacher R, Martine U, Closs EI, Filipowicz W (2006) Relief of microRNA-mediated translational repression in human cells subjected to stress. *Cell* **125,** 1111-1124.

Bhaumik D, Scott GK, Schokrpur S, Patil CK, Orjalo AV, Rodier F, Lithgow GJ, Campisi J (2009) MicroRNAs miR-146a/b negatively modulate the senescence-associated inflammatory mediators IL-6 and IL-8. *Aging* **1**.

Brazma A (2009) Minimum Information About a Microarray Experiment (MIAME)--successes, failures, challenges. *ScientificWorldJournal* **9,** 420-423.

Brazma A, Hingamp P, Quackenbush J, Sherlock G, Spellman P, Stoeckert C, Aach J, Ansorge W, Ball CA, Causton HC*, et al.* (2001) Minimum information about a microarray experiment (MIAME)-toward standards for microarray data. *Nat Genet* **29,** 365-371.

Brosh R, Shalgi R, Liran A, Landan G, Korotayev K, Nguyen GH, Enerly E, Johnsen H, Buganim Y, Solomon H*, et al.* (2008) p53-Repressed miRNAs are involved with E2F in a feed-forward loop promoting proliferation. *Mol Syst Biol* **4,** 229.

Campisi J (2003) Cancer and ageing: rival demons? *Nat Rev Cancer* **3,** 339-349.

Carthew RW, Sontheimer EJ (2009) Origins and Mechanisms of miRNAs and siRNAs. *Cell* **136,** 642-655.

Castoldi M, Schmidt S, Benes V, Noerholm M, Kulozik AE, Hentze MW, Muckenthaler MU (2006) A sensitive array for microRNA expression profiling (miChip) based on locked nucleic acids (LNA). *Rna* **12,** 913-920.

Chang MW, Grillari J, Mayrhofer C, Fortschegger K, Allmaier G, Marzban G, Katinger H, Voglauer R (2005) Comparison of early passage, senescent and hTERT immortalized endothelial cells. *Exp Cell Res* **309,** 121-136.

Cloonan N, Brown MK, Steptoe AL, Wani S, Chan WL, Forrest AR, Kolle G, Gabrielli B, Grimmond SM (2008) The miR-17-5p microRNA is a key regulator of the G1/S phase cell cycle transition. *Genome Biol* **9,** R127.

de Magalhaes JP, Budovsky A, Lehmann G, Costa J, Li Y, Fraifeld V, Church GM (2009) The Human Ageing Genomic Resources: online databases and tools for biogerontologists. *Aging Cell* **8,** 65-72.

Dimri GP, Hara E, Campisi J (1994) Regulation of two E2F-related genes in presenescent and senescent human fibroblasts. *J Biol Chem* **269,** 16180-16186.

Ebi H, Sato T, Sugito N, Hosono Y, Yatabe Y, Matsuyama Y, Yamaguchi T, Osada H, Suzuki M, Takahashi T (2009) Counterbalance between RB inactivation and miR-17-92 overexpression in reactive oxygen species and DNA damage induction in lung cancers. *Oncogene*.

Effros RB, Dagarag M, Spaulding C, Man J (2005) The role of CD8 T-cell replicative senescence in human aging. *Immunol Rev* **205,** 147-157.

Fehrer C, Brunauer R, Laschober G, Unterluggauer H, Reitinger S, Kloss F, Gully C, Gassner R, Lepperdinger G (2007) Reduced oxygen tension attenuates differentiation capacity of human mesenchymal stem cells and prolongs their lifespan. *Aging Cell* **6,** 745-757.

Ghildiyal M, Zamore PD (2009) Small silencing RNAs: an expanding universe. *Nat Rev Genet* **10,** 94-108.

Griffiths-Jones S, Saini HK, van Dongen S, Enright AJ (2008) miRBase: tools for microRNA genomics. *Nucleic Acids Res* **36,** D154-158.

Grillari J, Grillari-Voglauer R (submitted) Novel modulators of aging and longevity: small non-coding RNAs enter the stage. *Exp Gerontol*.

Hampel B, Fortschegger K, Ressler S, Chang MW, Unterluggauer H, Breitwieser A, Sommergruber W, Fitzky B, Lepperdinger G, Jansen-Durr P*, et al.* (2006) Increased expression of extracellular proteins as a hallmark of human endothelial cell in vitro senescence. *Exp Gerontol* **41,** 474-481.

He L, Thomson JM, Hemann MT, Hernando-Monge E, Mu D, Goodson S, Powers S, Cordon-Cardo C, Lowe SW, Hannon GJ, Hammond SM (2005) A microRNA polycistron as a potential human oncogene. *Nature* **435,** 828-833.

Hochberg Y, Benjamini Y (1990) More powerful procedures for multiple significance testing. *Stat Med* **9,** 811-818.

Hulsen T, de Vlieg J, Alkema W (2008) BioVenn - a web application for the comparison and visualization of biological lists using area-proportional Venn diagrams. *BMC Genomics* **9,** 488.

Hutter E, Unterluggauer H, Uberall F, Schramek H, Jansen-Durr P (2002) Replicative senescence of human fibroblasts: the role of Ras-dependent signaling and oxidative stress. *Exp Gerontol* **37,** 1165-1174.

Inomata M, Tagawa H, Guo YM, Kameoka Y, Takahashi N, Sawada K (2009) MicroRNA-17-92 down-regulates expression of distinct targets in different B-cell lymphoma subtypes. *Blood* **113,** 396-402.

Ivanovska I, Ball AS, Diaz RL, Magnus JF, Kibukawa M, Schelter JM, Kobayashi SV, Lim L, Burchard J, Jackson AL*, et al.* (2008) MicroRNAs in the miR-106b family regulate p21/CDKN1A and promote cell cycle progression. *Mol Cell Biol* **28,** 2167-2174.

Izzotti A, Calin GA, Steele VE, Croce CM, De Flora S (2009) Relationships of microRNA expression in mouse lung with age and exposure to cigarette smoke and light. *Faseb J* **23,** 3243-3250.

Jaffe EA, Nachman RL, Becker CG, Minick CR (1973) Culture of human endothelial cells derived from umbilical veins. Identification by morphologic and immunologic criteria. *J Clin Invest* **52,** 2745-2756.

Jeyapalan JC, Ferreira M, Sedivy JM, Herbig U (2007) Accumulation of senescent cells in mitotic tissue of aging primates. *Mech Ageing Dev* **128,** 36-44.

Kirkwood TB (2008) Understanding ageing from an evolutionary perspective. *J Intern Med* **263,** 117-127.

Knapen D, Vergauwen L, Laukens K, Blust R (2009) Best practices for hybridization design in two-colour microarray analysis. *Trends Biotechnol* **27,** 406-414.

Kulju KS, Lehman JM (1995) Increased p53 protein associated with aging in human diploid fibroblasts. *Exp Cell Res* **217,** 336-345.

Lal A, Kim HH, Abdelmohsen K, Kuwano Y, Pullmann R, Jr., Srikantan S, Subrahmanyam R, Martindale JL, Yang X, Ahmed F*, et al.* (2008) p16(INK4a) translation suppressed by miR-24. *PLoS ONE* **3,** e1864.

Laschober GT, Brunauer R, Jamnig A, Fehrer C, Greiderer B, Lepperdinger G (2009) Leptin receptor/CD295 is upregulated on primary human mesenchymal stem cells of advancing biological age and distinctly marks the subpopulation of dying cells. *Exp Gerontol* **44,** 57-62.

Lazuardi L, Herndler-Brandstetter D, Brunner S, Laschober GT, Lepperdinger G, Grubeck-Loebenstein B (2009) Microarray analysis reveals similarity between

CD8+CD28- T cells from young and elderly persons, but not of CD8+CD28+ T cells. *Biogerontology* **10,** 191-202.

Lepperdinger G, Berger P, Breitenbach M, Frohlich KU, Grillari J, Grubeck-Loebenstein B, Madeo F, Minois N, Zwerschke W, Jansen-Durr P (2008) The use of genetically engineered model systems for research on human aging. *Front Biosci* **13,** 7022-7031.

Li G, Luna C, Qiu J, Epstein DL, Gonzalez P (2009) Alterations in microRNA expression in stress-induced cellular senescence. *Mech Ageing Dev*.

Li N, Bates DJ, An J, Terry DA, Wang E (2009) Up-regulation of key microRNAs, and inverse down-regulation of their predicted oxidative phosphorylation target genes, during aging in mouse brain. *Neurobiol Aging*.

Lim LP, Lau NC, Garrett-Engele P, Grimson A, Schelter JM, Castle J, Bartel DP, Linsley PS, Johnson JM (2005) Microarray analysis shows that some microRNAs downregulate large numbers of target mRNAs. *Nature* **433,** 769-773.

Lukiw WJ (2007) Micro-RNA speciation in fetal, adult and Alzheimer's disease hippocampus. *Neuroreport* **18,** 297-300.

Maes OC, An J, Sarojini H, Wang E (2008) Murine microRNAs implicated in liver functions and aging process. *Mech Ageing Dev* **129,** 534-541.

Maes OC, An J, Sarojini H, Wu H, Wang E (2008) Changes in MicroRNA expression patterns in human fibroblasts after low-LET radiation. *J Cell Biochem*.

Maes OC, Sarojini H, Wang E (2009) Stepwise up-regulation of microRNA expression levels from replicating to reversible and irreversible growth arrest states in WI-38 human fibroblasts. *J Cell Physiol* **221,** 109-119.

Oender K, Trost A, Lanschuetzer C, Laimer M, Emberger M, Breitenbach M, Richter K, Hintner H, Bauer JW (2008) Cytokeratin-related loss of cellular integrity is not a major driving force of human intrinsic skin aging. *Mech Ageing Dev* **129,** 563-571.

Rodier F, Campisi J, Bhaumik D (2007) Two faces of p53: aging and tumor suppression. *Nucleic Acids Res* **35,** 7475-7484.

Saurwein-Teissl M, Lung TL, Marx F, Gschosser C, Asch E, Blasko I, Parson W, Bock G, Schonitzer D, Trannoy E, Grubeck-Loebenstein B (2002) Lack of antibody production following immunization in old age: association with

CD8(+)CD28(-) T cell clonal expansions and an imbalance in the production of Th1 and Th2 cytokines. *J Immunol* **168,** 5893-5899.

Smyth GK (2004) Linear models and empirical bayes methods for assessing differential expression in microarray experiments. *Stat Appl Genet Mol Biol* **3,** Article3.

Smyth GK, Michaud J, Scott HS (2005) Use of within-array replicate spots for assessing differential expression in microarray experiments. *Bioinformatics* **21,** 2067-2075.

Smyth GK, Speed T (2003) Normalization of cDNA microarray data. *Methods* **31,** 265-273.

Stefani G, Slack FJ (2008) Small non-coding RNAs in animal development. *Nat Rev Mol Cell Biol* **9,** 219-230.

Stockl P, Hutter E, Zwerschke W, Jansen-Durr P (2006) Sustained inhibition of oxidative phosphorylation impairs cell proliferation and induces premature senescence in human fibroblasts. *Exp Gerontol* **41,** 674-682.

Sturn A, Quackenbush J, Trajanoski Z (2002) Genesis: cluster analysis of microarray data. *Bioinformatics* **18,** 207-208.

Takakura S, Mitsutake N, Nakashima M, Namba H, Saenko VA, Rogounovitch TI, Nakazawa Y, Hayashi T, Ohtsuru A, Yamashita S (2008) Oncogenic role of miR-17-92 cluster in anaplastic thyroid cancer cells. *Cancer Sci* **99,** 1147-1154.

Wagner W, Horn P, Castoldi M, Diehlmann A, Bork S, Saffrich R, Benes V, Blake J, Pfister S, Eckstein V, Ho AD (2008) Replicative senescence of mesenchymal stem cells: a continuous and organized process. *PLoS ONE* **3,** e2213.

Wieser M, Stadler G, Jennings P, Streubel B, Pfaller W, Ambros P, Riedl C, Katinger H, Grillari J, Grillari-Voglauer R (2008) hTERT alone immortalizes epithelial cells of renal proximal tubules without changing their functional characteristics. *Am J Physiol Renal Physiol* **295,** F1365-1375.

Willenbrock H, Salomon J, Sokilde R, Barken KB, Hansen TN, Nielsen FC, Moller S, Litman T (2009) Quantitative miRNA expression analysis: comparing microarrays with next-generation sequencing. *Rna* **15,** 2028-2034.

Williams AE, Perry MM, Moschos SA, Lindsay MA (2007) microRNA expression in the aging mouse lung. *BMC Genomics* **8,** 172.

Woods K, Thomson JM, Hammond SM (2007) Direct regulation of an oncogenic micro-RNA cluster by E2F transcription factors. *J Biol Chem* **282,** 2130-2134.

Wurmbach E, Yuen T, Sealfon SC (2003) Focused microarray analysis. *Methods* **31,** 306-316.

Yan HL, Xue G, Mei Q, Wang YZ, Ding FX, Liu MF, Lu MH, Tang Y, Yu HY, Sun SH (2009) Repression of the miR-17-92 cluster by p53 has an important function in hypoxia-induced apoptosis. *Embo J.*

Figure legends

Figure 1: Microarray analysis of differential expression and enrichment of regulated miRNAs in replicative and organismal aging. (a) Size-adjusted Venn diagram depicting the intersection of regulated miRNAs from replicative and organismal aging models: the upper, yellow circle represents 5 miRNAs that were found significantly regulated (false discovery rate adjusted p-value < 0.05) in at least 3 out of the 4 replicative models. Only miRNAs with uniform up- or down-regulation in all models were considered. For organismal aging experiments 34 miRNAs were significantly regulated (FDR adjusted p-value < 0.05) in at least 2 out of 3 models, indicated by the lower, purple circle. (b) The intersection contains three miRNAs of the miR-17-92 cluster, namely miR-17, miR-19b and miR-20a, as well as miR-106a of the paralogous miR-106a-363 cluster. The individual “old versus young” ratios for these miRNAs, calculated from microarray data, are depicted in a barchart. (c) Fold changes in transcription of young versus old based on microarrays are given for all members of the miR-17-92 cluster as well as selected miRNAs from paralogous clusters together with 5’ seed sequences. Adjusted p-values < 0.05 are marked in bold and underlined format, indicating statistically significant regulation.

Figure 2: Quantitative real-time PCR of miRNAs and the published target p21/CDKN1A. (a) Down-regulation of miR-17, miR-19b, miR-20a and miR-106a in microarray experiments was validated by quantitative PCR analysis. miRNA expression values were normalized to GAPDH levels for each experiment (n=8; $p<0.05$, one sample t-test with $\mu_0 = 0$) (b) Messenger RNA levels of p21/CDKN1A were analysed by qPCR, and normalized to GAPDH expression levels (n=8; $p<0.05$, one sample t-test with $\mu_0 = 0$). Increased p21 levels were observed in senescence and organismal aging indicating negative correlation to transcription of members of the miR-17-92 cluster.

HDF: human diploid fibroblasts, HUVEC: human umbilical vein endothelial cells, RPTEC: renal proximal tubular epithelial cells, MSC: bone marrow derived mesenchymal stem cells, FSK: human foreskin, GAPDH: Glycerinaldehyd-3-phosphat-Dehydrogenase.

Figure S1: Characteristization of the analyzed model systems of aging. Representative growth curves of HUVECs (a), fibroblasts (b), and RPTECs (c) are presented, indicating replicative growth arrests at late passages. Senescence at the time of harvest was confirmed by >95% positive cells after senescence-associated β-galactosidase staining. Furthermore, morphological characteristics were typical for senescent cells. Representative images of cells are given below the growth curves. (d) Replicatively exhausted ($CD28^-$) versus non-exhausted $CD8^+$ T cells ($CD28^+$) were separated after taking blood samples by magnetic-activated cell separation and identity and purity of the populations was confirmed by flow cytometry using antibodies against CD28. (e) Donor characteristics regarding the age range, the mean age for young and old donors as well as the total number (n) of donors for T cells, mesenchymal stem cell, and foreskin specimens are summarized.

Figure S2: Experimental design of differential miRNA analysis. (a) Depending on the individual experimental setup (the number of biological replicates and the contrasts that were of interest) an appropriate hybridization strategy was chosen for each aging model system. Experimental designs of all hybridizations are depicted using a visualization scheme introduced by (Knapen *et al.*, 2009). In addition to the number of biological and dye swap replicates, also the Array Express accession numbers are given, which allow access to the entire set of raw and normalized microarray data. (b) According to the chosen design, total RNA was hybridized to Sanger miRBase v8.0 or v9.2 LNA microarrays and scanned as described in the supporting material and methods section. (c) For data analysis array spot intensities were first $\log_2$ transformed, background corrected using the normexp algorithm and lowess normalized using R in combination with LIMMA (Linear Models for Microarray Data, Bioconductor). A representative graph before and after normalization is shown. Normalized data were then visualized and clustered using Genesis software from TU Graz, and tested for differential expression by fitting linear models to the data and applying moderated t-statistics and false discovery rate adjustment. (d) Data regarding differential expression of miRNAs were confirmed using LNA qPCR. In addition, expression of selected mRNA targets of the regulated miRNAs was measured using SYBR Green qPCR. (e) Comprehensive protocols and data for all miRNA microarray experiments were submitted to Array Express

(http://www.ebi.ac.uk/microarray-as/ae/) according to the Minimal Information about Microarray Data (MIAME) submission guidelines.

Figure S3: Heatmap visualization and clustering of miRNA expression data. (a) The fold changes in expression (old versus young) of the miRNAs were log_2-transformed and visualized in a heatmap where yellow color indicates up-regulation in aged or replicated samples, while blue corresponds to down-regulation (maximum yellow/blue color intensities were manually set to three). Experiments as well as miRNAs were subjected to hierarchical clustering (complete linkage distance calculation) indicated by dendrograms. (b) Linked expression view of log_2 transformed fold changes in miRNA expression (old vs. young or replicated vs young) is shown. The pink line, corresponding to the median expression change in each model, indicates that the majority of miRNAs exhibits no regulation (log_2 fold change = 0). The entire set of miRNAs was filtered for miRNAs with altered transcription (+/- 0.4 log_2-fold change) in the majority of the single model systems resulting in 17 miRNAs. (c) A heatmap of these 17 miRNAs after hierarchical clustering is shown. Clustering yielded a 9 miRNAs comprising cluster characterized by consistent down-regulation in the majority of experiments. miRNAs generated from a single primary transcript at 13q31.3 – the miR-17-92 cluster of miRNAs – (or paralogous clusters 106a-363 and 106b-25) were found to be enriched among these miRNAs and are highlighted by black arrows.

Table S1: Overview on total numbers of transcribed miRNA as well on miRNAs detected as differentially transcribed. From a total set of 806 miRNAs, those with transcription levels 2-fold above background were considered present and subjected to statistical testing. miRNAs were considered to be differentially transcribed if a false discovery rate adjusted p-value of below 0.05 was found.
HUVEC: human umbilical vein endothelial cells; HDF: normal human diploid fibroblasts; RPTEC: renal proximal tubular epithelial cells; MSC: bone marrow derived mesenchymal stem cells; FSK: human foreskin; RA: replicative aging; OA: organismal aging

Table S2: Compilation of all regulated miRNAs in all experimental systems (provided as MS Excel file only). Each model system is presented in a separate excel sheet.

Table S3: Experimentally validated target mRNAs of the miR-17-92 cluster. References within the table correspond to following within the main text:

(1) Cloonan N, Brown MK, Steptoe AL, Wani S, Chan WL, Forrest AR, Kolle G, Gabrielli B, Grimmond SM (2008) The miR-17-5p microRNA is a key regulator of the G1/S phase cell cycle transition. *Genome Biol* **9,** R127.

(2) Hossain A, Kuo MT, Saunders GF (2006) Mir-17-5p regulates breast cancer cell proliferation by inhibiting translation of AIB1 mRNA. *Mol Cell Biol* **26,** 8191-8201.

(3) Ivanovska I, Ball AS, Diaz RL, Magnus JF, Kibukawa M, Schelter JM, Kobayashi SV, Lim L, Burchard J, Jackson AL*, et al.* (2008) MicroRNAs in the miR-106b family regulate p21/CDKN1A and promote cell cycle progression. *Mol Cell Biol* **28,** 2167-2174.

(4) Landais S, Landry S, Legault P, Rassart E (2007) Oncogenic potential of the miR-106-363 cluster and its implication in human T-cell leukemia. *Cancer Res* **67,** 5699-5707.

(5) Lewis BP, Shih IH, Jones-Rhoades MW, Bartel DP, Burge CB (2003) Prediction of mammalian microRNA targets. *Cell* **115,** 787-798.

(6) O'Donnell KA, Wentzel EA, Zeller KI, Dang CV, Mendell JT (2005) c-Myc-regulated microRNAs modulate E2F1 expression. *Nature* **435,** 839-843.

(7) Pichiorri F, Suh SS, Ladetto M, Kuehl M, Palumbo T, Drandi D, Taccioli C, Zanesi N, Alder H, Hagan JP*, et al.* (2008) MicroRNAs regulate critical genes associated with multiple myeloma pathogenesis. *Proc Natl Acad Sci U S A* **105,** 12885-12890.

(8) Pickering MT, Stadler BM, Kowalik TF (2009) miR-17 and miR-20a temper an E2F1-induced G1 checkpoint to regulate cell cycle progression. *Oncogene* **28,** 140-145.

(9) Volinia S, Calin GA, Liu CG, Ambs S, Cimmino A, Petrocca F, Visone R, Iorio M, Roldo C, Ferracin M*, et al.* (2006) A microRNA expression signature of human solid tumors defines cancer gene targets. *Proc Natl Acad Sci U S A* **103,** 2257-2261.

(10) Yu Z, Wang C, Wang M, Li Z, Casimiro MC, Liu M, Wu K, Whittle J, Ju X, Hyslop T*, et al.* (2008) A cyclin D1/microRNA 17/20 regulatory feedback loop in control of breast cancer cell proliferation. *J Cell Biol* **182,** 509-517.

(11) Li G, Luna C, Qiu J, Epstein DL, Gonzalez P (2009) Alterations in microRNA expression in stress-induced cellular senescence. *Mech Ageing Dev*.

Overview on Supporting Information

Table S1

Table S2

Table S3

Fig. S1

Fig. S2

Fig. S3

Legends are included in the fig. legends section above.

Supporting materials and methods

Supporting Material and Methods

Cell Lines

Human Dermal Fibroblasts (HDFs)

Normal human fibroblasts were isolated from skin biopsies of two different healthy causcasian patients, a 41-years old female (HDF-1) and a 16-years old male (HDF-5). HDF-5 and HDF-1 cells were cultivated in DMEM/HAM's F-12 medium (Biochrom KG, Berlin, Germany) supplemented with 10% fetal calf serum (FCS) 4 mM L-glutamine (Sigma) and Primocin antibiotics (100 µg/mL). Cells were grown at 37 °C in ambient atmosphere containing 5% CO_2. Until confluence was reached HDF cells were routinely passaged at 1:4 or 1:3 split ratios. Upon decrease in growth rate and entry of irreversible growth arrest split ratio was changed to 1:2 and after cells had stopped dividing, fresh medium was added every 7 days. HDF-1 cells reached senescence after 54 population doublings (PDLs), while HDF-5 cells had stopped growing after 72.7 PDLs.

Human Umbilical Vein Endothelial Cells (HUVECs)

Endothelial cells were isolated from human umbilical veins (Jaffe *et al.*, 1973) and cultured in Endothelial Cell Basal Medium (Lonza) supplemented with EGM Single Quots (Lonza), containing hEGF 0.5 mL, hydrocortisone 0.5 mL, GA-1000 0.5 mL, BBE 2.0 mL, FBS 10.0 mL. The cells were subcultured by trypsinization with trypsin-EDTA (Gibco Life Technologies, Vienna, Austria), seeded on cell culture dishes coated with 0.2% gelatine and grown at 37 °C at ambient atmosphere containing 5% CO_2. Cells were passaged at a ratio of 1:5 in regular intervals. At later passages, the splitting ratio was reduced to 1:3 and 1:2, respectively. Cells were passaged before reaching 70-80% confluency. PDL were estimated using the following equation: PDL = $(\log_{10}(F)-\log_{10}(I)) / 0.301$ (where F is the number of cells at the end of one passage, and I the number of cells that were seeded at the beginning of one passage). After roughly 50 population doublings, cells had reached growth arrest.

Renal Proximal Tubular Epithelial Cells (RPTECs)

RPTECs were cultivated as recently reported (Wieser *et al.*, 2008). In brief, within 24 hours after surgery tissue from the renal cortex was fragmented and incubated at 37°C for 15-20 minutes in DMEM/Ham's F12 (1:1) (Biochrom KG, Berlin, Germany)

containing 1 mg/mL collagenase type IV (PAN-BioTech GmbH, Aidenbach, Germany) and 1 mg/mL trypsin-inhibitor (Sigma, Vienna, Austria). After being passed through a 105 µm nylon mesh the filtrate was centrifuged, washed twice with phosphate buffered saline (PBS), resuspended in medium and dispensed into roux-flasks (Nunc, Wiesbaden, Germany). 24 hours thereafter medium was changed. The initial passage of confluent cells after 3-5 days was considered as PDL zero. Cells were passaged (1:2 to 1:4) at confluence, using 0.25% trypsin/0.02% EDTA, which was inactivated with 1 mg/mL trypsin-inhibitor. Cumulative PDL was calculated as a function of passage number and split ratio. Medium consisted of DMEM/Ham's F12 (1:1) supplemented with 4 mM L-glutamine, 10 mM HEPES buffer, 5 pM triiodothyronine, 10 ng/mL recombinant human EGF, 3.5 µg/mL ascorbic acid, 5 µg/mL transferrin, 5 µg/mL insulin, 25 ng/mL prostaglandin E1, 25 ng/mL hydrocortisone and 8.65 ng/mL sodium selenit (all from Sigma). For RPTEC/TERT1 the medium was supplemented with 100 µg/mL G418 (Sigma).

In vivo specimens

Mesenchymal Stem Cells

MSC were isolated from the iliac crest of systemically healthy individuals (young donors, n=4, mean age 18, range 5-23; elderly donors, n=4, mean age 66, range 47-78) which had been harvested for reconstructive bone surgery of defects within other areas of the body as described previously (Fehrer *et al.*, 2007). Briefly, a small biopsy of substantia spongiosa osseum, which otherwise would have been discarded based on necessary bone for molding and recontouring prior to insertion into the recipient site was taken to further investigation under an Institutional Review Board-approved protocol after having obtained patients' written consent. After surgery, the bone was transferred into minimal essential medium (MEM) supplemented with 20% heat-inactivated fetal calf serum, 100 units/mL penicillin, 100 µg/mL streptomycin (growth medium) for transportation from the operation theatre to the clean room at room temperature. The biopsies were fragmented and marrow cells were isolated from pieces (20-100 mm^3) by centrifugation (400*xg*, 1 minute). After centrifugation, the remaining pieces were treated with collagenase (2.5 mg/mL in MEM) for 2-3 hours at 37°C, 20% O_2 and 5% CO_2. Thereafter, the specimen was again centrifuged (400*xg*, 1 minute). Cells were resuspended and loaded on a Ficoll-Paque Plus® gradient and centrifuged at 2,500*xg* for 30 minutes. Cells were harvested from the

interphase (density <1.075 g/mL), washed and collected by centrifugation (1,500*xg*, 15 minutes). Cells were cultured at a density of 0.2 – 0.5 x 10^6 cells/cm^2 at 5% CO_2 and 37°C and 3% O_2 (Thermo Electron Forma Series II, 3110). After 24 hours, the non-adherent cell fraction was removed by washing twice with phosphate-buffered saline (PBS). After the primary culture had reached approximately 30 – 50% confluence, cells were washed twice with PBS, and subsequently treated with 0.05% trypsin / 1 mM EDTA for 3 – 5 minutes at 37°C. Cells were harvested, washed in MEM and further expanded at a density of 50 cells/cm².

T cells

Isolation of $CD8^+CD28^+$ and $CD8^+CD28^-$ T cells from peripheral blood of apparently healthy young (<35y, n=6, mean age 29, range 26-35) and elderly (>65y, n=10, mean age 72, range 66-87) donors was performed by preparing peripheral blood mononuclear cells (PBMCs) by Ficoll-Paque PLUS (Amershan Biosciences) density gradient centrifugation as approved by the local ethics committee. $CD8^+$ T cells were negatively selected from the obtained PBMC fraction by applying the magnetic separation protocol $CD8^+$ T cell isolation kit II (depleting CD4, CD14, CD16, CD19, CD36, CD56, CD123, TCRγ/δ and CD235a, Miltenyi Biotec) according to the manufacturer's instructions. Subsequently, purified $CD8^+$ T cells were stained with an Allophycocyanin (APC)-conjugated αCD28 monoclonal antibody (mAb) and split into $CD8^+CD28^+$ and $CD8^+CD28^-$ T cell populations using αAPC MicroBeads (Miltenyi Biotec) by passing the cell suspension through a positive selection column (LS; Miltenyi Biotec) mounted in a magnetic field. The $CD8^+CD28^-$ T cell fraction was then reincubated with αAPC MicroBeads and run over a fresh LS-column to increase purity. For phenotypic analysis, purified T cell fractions were labelled with a combination of mAbs (αTCRαβ-FITC, αCD16-PE, αCD4-PerCP, αCD8-PE-Cy7, αCD28-APC and αCD3-APC-Cy7; all BD Biosciences - Pharmingen) and analyzed on a FACSCanto II (BD Biosciences) revealing that the described isolation protocol yields population homogeneities of >95%.

Foreskin

Foreskins from donors of different age were frozen in liquid nitrogen and grinded in a mortar. Each sample was lysed in 2 mL Trizol (Invitrogen), and RNA was prepared as described below.

Microarray Analysis of miRNA Expression

RNA Extraction

For two channel microarray analysis of miRNA expression 0.5 to 1 µg of high quality total RNA were used for labeling. Briefly, total RNA was extracted from cells using Trizol reagent (Invitrogen, CA). 10^6 - $5*10^6$ cells were pelleted at 900*xg* for 10 minutes and homogenized in 1 mL Trizol (Invitrogen) by vigorous mixing on a vortex (15 sec) followed by incubation at RT for 5 minutes. 200 µL Chloroform were added per 1 mL Trizol, and mixed on a vortex for 15 seconds followed by 3-minute incubation at room temperature. Samples were then centrifuged at 12000*xg* and 4℃ for 15 minutes. The upper (aqueous) phase was transferred to a new RNase-free tube and precipitated with 0.5 mL isopropanol (100%, room temperature) per 1 mL initial volume of Trizol. Samples were incubated 10 minutes at room temperature, followed by centrifugation at 12000*xg* for 10 minutes (4℃). The supernatant was discarded and the RNA pellet was washed with 1 mL 75% EtOH (room temperature), and subsequently centrifuged at 7500*xg* for 5 minutes. Ethanol was discarded and the RNA pellet was dried for 10 minutes at room temperature in a fume hood. For resuspension of RNA pellets 20 µL RNase-free water were used. To increase solubility resuspended RNA was incubated at 60℃ for 10 minutes. RNA concentration was quantitated using NanoDrop (ThermoScientific, Wilmington, USA) and quality was assessed by testing ribosomal RNA integrity (RNA 6000 Nano Kit, Agilent, Germany). RNA with integrity numbers (RIN) equal or greater than 7 were subsequently stored at -80℃.

In-house LNA MiRNA Chips (MRC)

MiRNA Microarrays were spotted on epoxy-coated Nexterion glass slides (Schott AG, Germany) using the MicroGrid II (Zinsser Analytic, Germany) Microarrayer and miRBase version 8.0 or 9.2 locked nucleic acid probe set (Exiqon Inc., Denmark), respectively. The spotted probe set consisted of 559 human and 170 murine miRNAs as well as of 77 miRPlus (intellectual property of Exiqon Inc, Denmark) sequences, which were spotted in 8 replicates on each array. Spotting was performed according to the supplier´s instruction manual and recommendations provided by Exiqon. Subsequently, in order to assure the quality of spotted miRNA microarrays, scanning of all slides was performed. Weak buffer autofluorescence confirmed the presence of more than 98% of spots.

RNA Hybridization

For two channel microarray analysis of miRNA expression 0.5 to 1 µg of high quality total RNA were used for labelling using the miRCURY LNA miRNA Array labelling kit (Exiqon, Inc; unless mentioned, all reagents were purchased from Exiqon). Following calf intestinal phosphatase cleavage for 30 minutes at 37℃, labelling with Cy3 and Cy5 fluorescent dyes was performed in a PCR thermocycler at 16℃ for 1 hour followed by incubation for 15 minute at 65℃ to stop the reaction. Cy3 and Cy5 labelled samples were pooled and mixed with nuclease free water and 2x hybridization buffer to yield 90 µL of hybridization sample in 1x hybridization buffer. Prior to hybridization samples were denatured at 95℃ for 2 minutes and snap cooled on ice. RNA samples were then hybridized at 60℃ for 16 hours to in-house spotted LNA miRNA chips using a TECAN HS 400 hybridization station (Tecan, Switzerland). Following hybridzation, washing and drying of LNA miRNA microarrays, arrays were immediately scanned using a GenePix 4000B laser scanner and GenePixPro 4.1 software (Axon Instruments). Cy3 dye was scanned at 532nm and Cy5 at 635nm. Scanning settings were adjusted to 10µM resolution and averaging per 1 line. Photomultiplier settings were adjusted individually for Cy3 and Cy5 according to the results from preview scans.

Microarray data analysis

R/Bioconductor

Intensity values for each spot were extracted using GenePix 4.1 software and inserted into R. Bioconductor and the “Linear models for microarray data analysis” package (Smyth, 2004) were used for the calculation of M-A values for each spot, where M stands for logarithmic red/green ratio ($\log_2$[R/G]) and A for average $\log_2$ intensity ($\log_2$[R*G]*0.5). The MA dataset of each array was background corrected using normexp algorithm and lowess (local weighted linear regression) normalized. Normalized data compared to raw data was visualized using MA and PrintTip Boxplot diagnostic plots as well as density plots (Smyth & Speed, 2003). Subsequently, in order to calculate fold changes in miRNA expression in replicated or aged samples, the 8 replicate spots of each miRNA per array were correlated and linear models

were fitted to the data (Smyth *et al.*, 2005). Contrast matrices were defined individually for each experiment, and moderated hypothesis tests (moderated t-statistic) were performed for the contrasts of interest. The data was then adjusted for multiple testing (p-adj.), by controlling the false discovery rate according to a method of Benjamini and Hochberg. All miRNAs were then ranked in terms of their adjusted p-values and a cut-off of p-adj. ≤ 0.05 was imposed (Hochberg & Benjamini, 1990).

Clustering and Visualization of Array Data

In order to cluster and visualize $\log_2$-transformed ratios (LFC) in a heatmap, the freely available Genesis software (Sturn *et al.*, 2002) was used. The LFCs of 347 miRNAs (corresponding to the intersection between miRBase v8.0 and v9.2 arrays, plus 77 proprietary miRPlus sequences from Exiqon) were inserted in Genesis and, in a second step, filtered for miRNAs which exhibited $\log_2$-fold changes greater than the average fold change plus 1.5 fold the standard deviation in at least 4 out of 7 experiments (corresponding to a LFC of +/- 0.4).

For identification and visualization of miRNAs regulated in both replicative and organismal aging, the web-based BioVenn application was used (Hulsen *et al.*, 2008).

Quantitative miRNA LNA-PCR and mRNA PCR

Isolated total RNA from all samples was brought to a concentration of 10 ng/µL and 2 ng/µL in RNAse-free water and quantitative PCR (qPCR) was performed on selected miRNAs and on the internal housekeeping gene glyceraldehyde-3-phosphate dehydrogenase (GAPDH) as well as p21/CDKN1A using a RotorGene 6000 Real-Time Cycler (Qiagen, Germany).

For each miRNA, 9 ng total RNA preparation (4.5 µL) were reverse transcribed in a LNA first strand cDNA synthesis reaction using the miRCURY LNA miRNA PCR System (Exiqon, Inc.) in combination with validated LNA PCR primers (Exiqon, Inc.). Subsequent to 1:10 dilution of the obtained cDNA, 4 µL were used for quadruplicate miRNA PCR reaction according to recommendations of the manufacturer. For GAPDH housekeeping gene as well as p21/CDKN1A, 70 ng total RNA were reverse transcribed using MMLV-reverse transcriptase (Finnzymes, Finnland) and random hexamer primers. Following 1:3 dilution in nuclease-free water, 1 µL cDNA was qPCR amplified in quadruplicate using SensiMix Plus SYBR Green (Quantace,

Germany) and specific primers (250 pM final concentration). To ensure appropriate size of the amplification products, melting points were determined after each amplification. For copy number determination of mRNAs, internal standards were included in each run. These were derived from PCR amplification from human cDNA and subsequent PCR product purification (Promega) and quantitation. Six standards in the range from 10^8 to 10^3 copies/µL were included in each run. The resulting standard curve was calculated in Rotor-Gene 6000 Series Software 1.7 and used for quantification of copy numbers of mRNA targets.

(a)

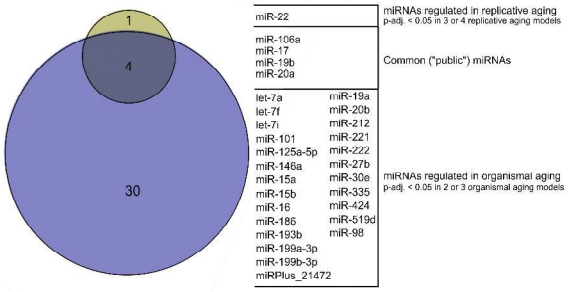

(b)

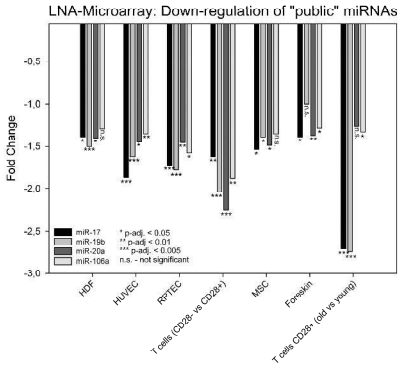

(c)

microRNA ID	Cluster	Seed Sequence	Replicative Aging				Organismal Aging		
			HDF	HUVEC	RPTEC	T cells CD28⁻ vs CD28⁺	MSC	FSK	T cells CD28⁺ old vs young
miR-17	miR-17~92	**AAAGUG**	**-1,39**	**-1,73**	**-1,87**	**-1,63**	**-1,54**	**-1,39**	**-2,71**
miR-18a		**AAAGUG**	-1,10	-1,28	-1,34	-1,40	-1,09	1,02	**-1,24**
miR-19a		GUGCAA	-1,08	1,05	**-1,73**	-0,15	**-1,69**	**-1,33**	**-1,96**
miR-19b		GUGCAA	**-1,50**	**-1,78**	**-1,62**	**-1,85**	**-1,39**	-1,00	**-2,74**
miR-20a		**AAAGUG**	**-1,40**	**-1,45**	**-1,45**	**-2,24**	**-1,49**	**-1,37**	-1,26
miR-92a		AUUGCA	-1,09	-1,75	n/a	**-1,39**	1,05	-1,16	**1,68**
miR-106a	miR-106a~363	**AAAGUG**	-1,29	**-1,58**	**-1,35**	**-1,89**	-1,35	**-1,28**	**-1,33**
miR-20b		**AAAGUG**	-1,01	-1,08	-1,67	-1,43	1,02	**-1,37**	**-2,14**
miR-106b	miR-106b~25	**AAAGUG**	-1,33	-1,26	**-1,17**	-1,23	-1,31	-1,05	**-1,68**
miR-519d	miR-371 cluster	U**AAAGUG**C	-1,35	-1,20	1,01	-0,05	**-1,81**	-1,15	**-2,60**

p-adj. < 0.05

297x210mm (600 x 600 DPI)

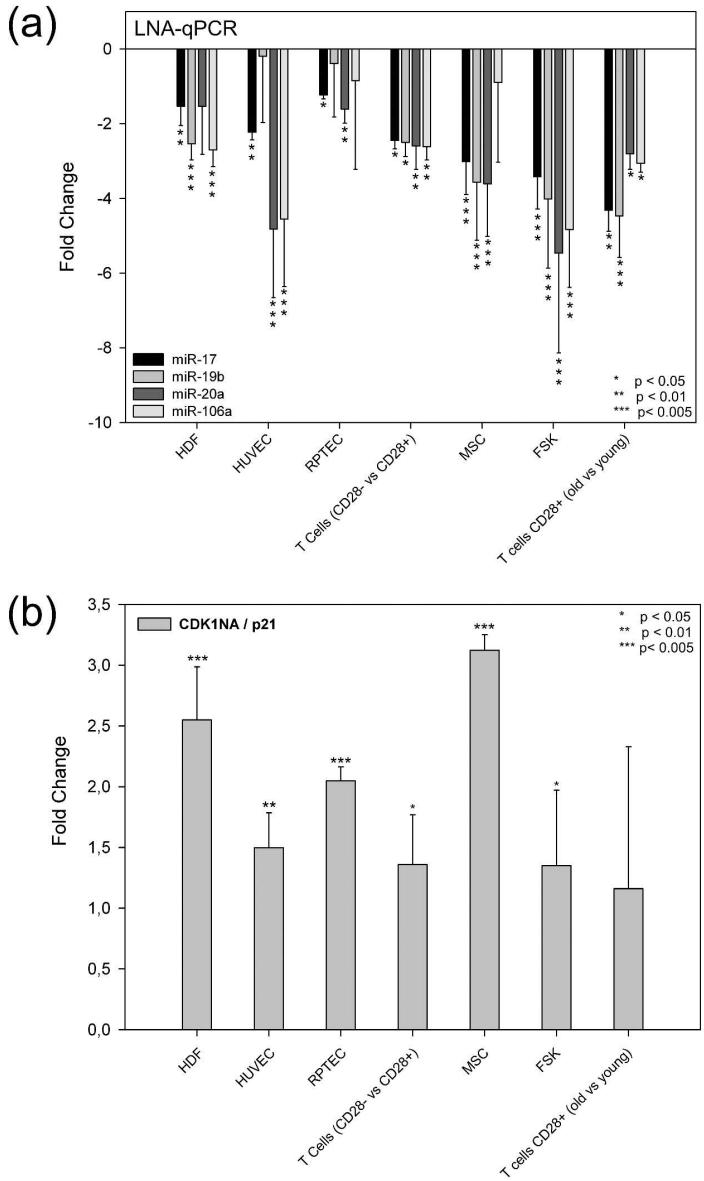

108x182mm (600 x 600 DPI)

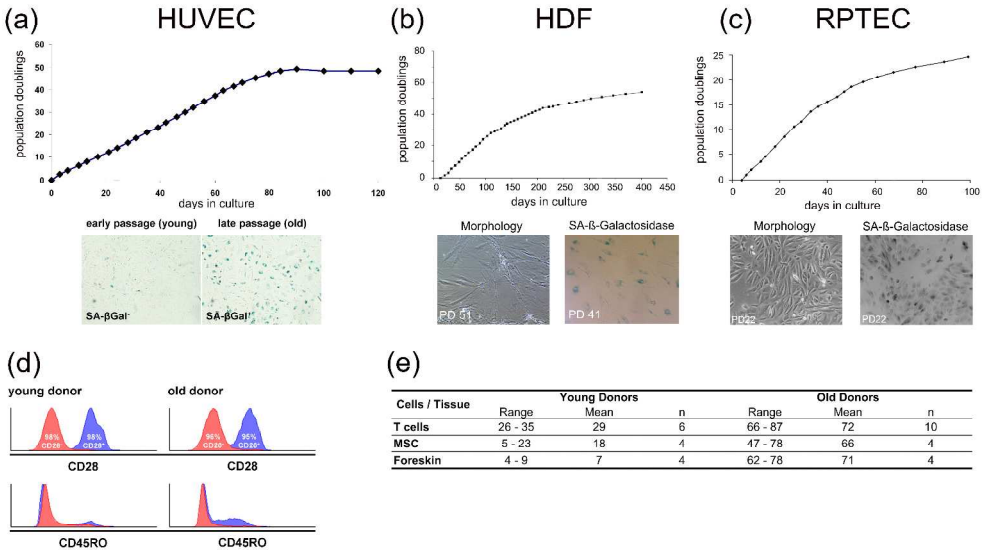

(d)

(e)

Cells / Tissue	Young Donors			Old Donors		
	Range	Mean	n	Range	Mean	n
T cells	26 - 35	29	6	66 - 87	72	10
MSC	5 - 23	18	4	47 - 78	66	4
Foreskin	4 - 9	7	4	62 - 78	71	4

299x165mm (600 x 600 DPI)

Biological Question = Changes in microRNA Expression in Human Aging

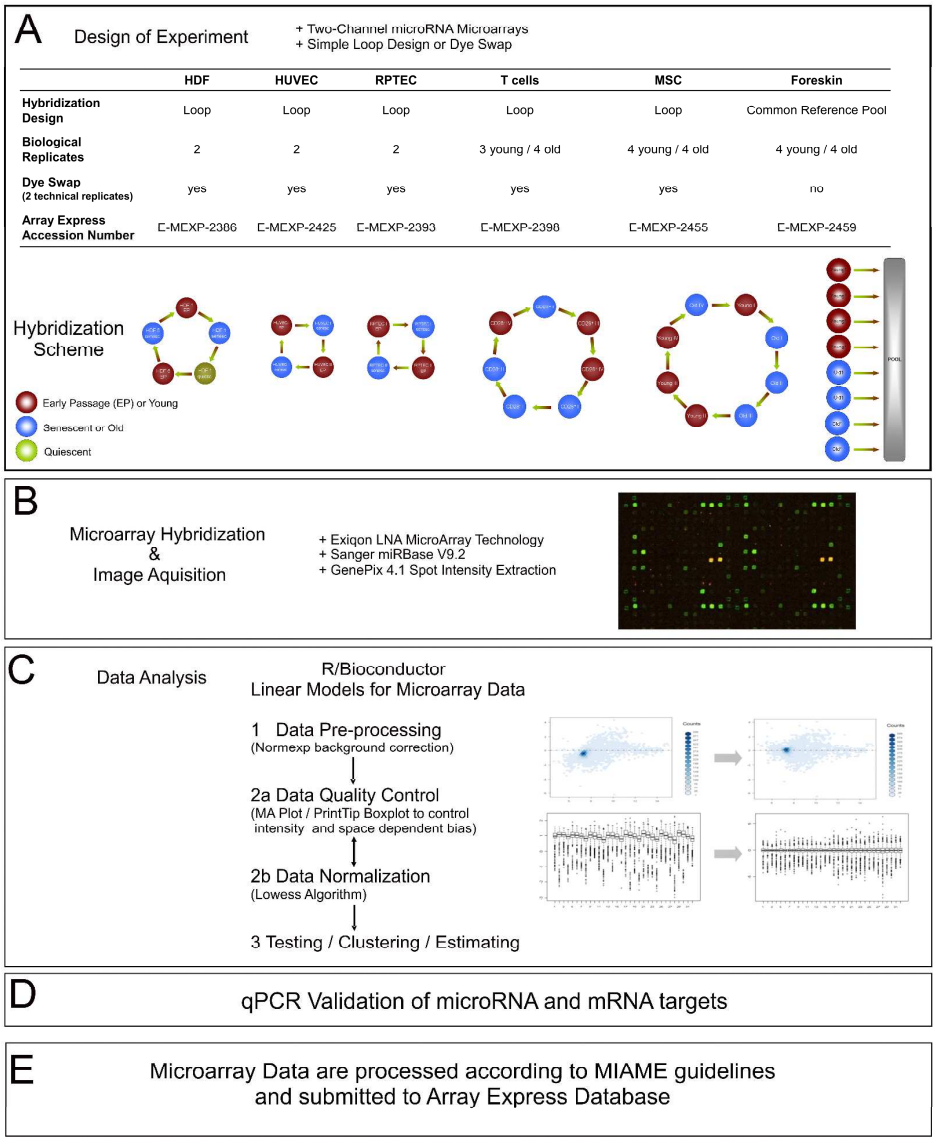

208x263mm (600 x 600 DPI)

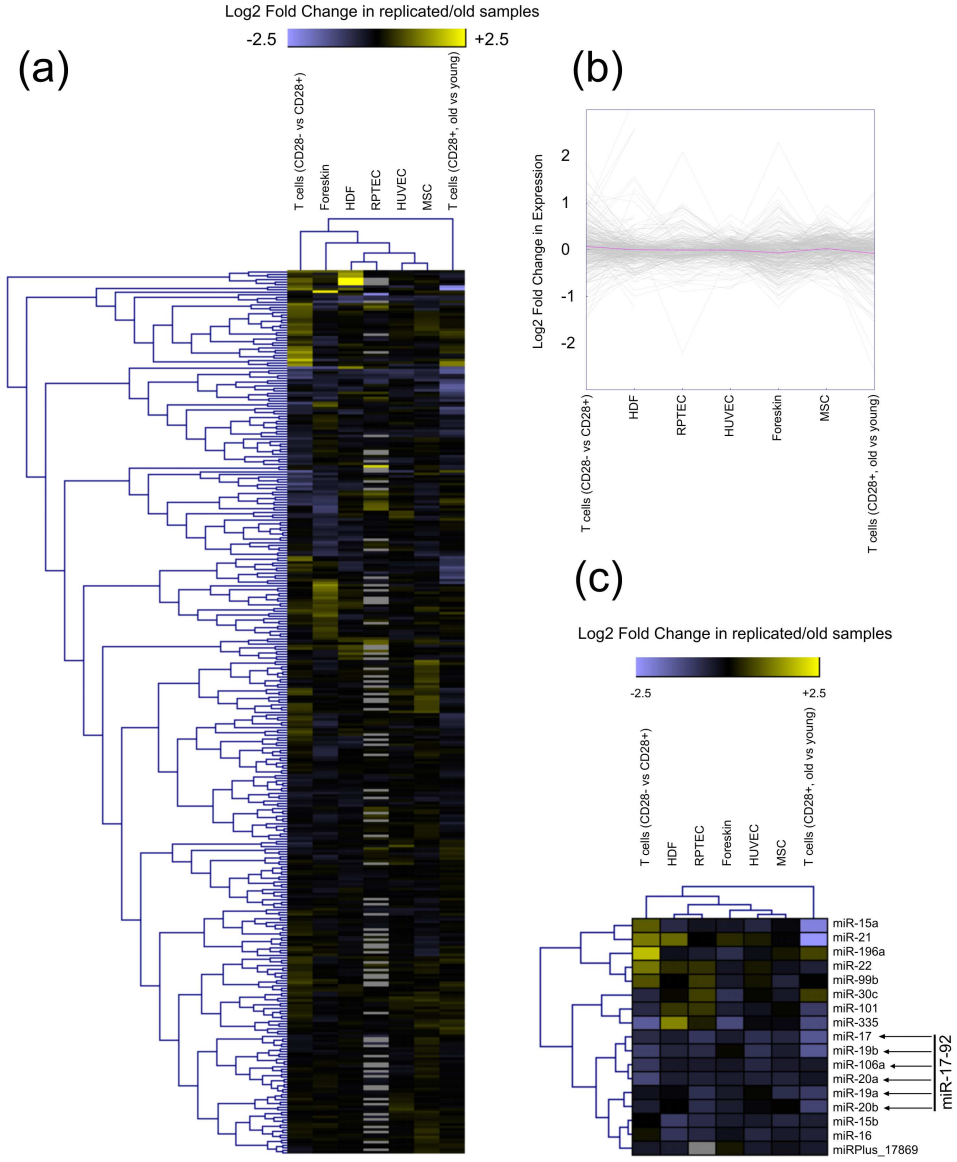

131x152mm (600 x 600 DPI)

	Replicative Aging				Organismal Aging		
Contrast	replicated versus early passage				old donor versus young donor		
Tissue Type / Cell Type	**Human Dermal Fibroblasts**	**Human umbilical vein endothelial cells**	**Renal proximal tubular epithelial cells**	**T cells $CD28^+$ / $CD28^-$**	**Mesenchymal Stem Cells**	**Foreskin**	**T cells $CD28^+$**
Abbreviation	HDF	HUVEC	RPTEC	T cells $CD28^-$ vs $CD28^+$	MSC	FSK	T cells $CD28^+$ old vs. young
Transcribed* microRNAs	248	128	250	237	584	271	237
Differentially transcribed microRNAs	51 (21%)	18 (14%)	73 (29%)	36 (15%)	19 (3%)	147 (54%)	49 (21%)
Up-regulated microRNAs	33	7	38	11	2	64	8
Down-regulated microRNAs	18	11	35	25	17	83	41

* Intensity > Average background + 2x standard deviation

201x65mm (600 x 600 DPI)

Exiqon Reporter ID (v9.2)	Reporter Name	log2 Fold Change
28351	mmu-miR-762	2.886
17890	miRPlus_17890	3.254
21472	miRPlus_21472	2.560
27561	miRPlus_27561	2.594
17558	hsa-miR-663	2.785
13511	hsa-miR-210	1.571
11130	hsa-miR-498	1.507
17399	mmu-miR-501-3p	1.781
5740	hsa-miR-21	1.031
17836	hsa-miR-30b*	1.071
17423	hsa-miR-584	1.766
13180	hsa-miR-483-3p	1.287
17848	miRPlus_17848	-1.237
21757	hsa-miR-766	1.775
17885	hsa-miR-886-5p	-1.171
17321	mmu-miR-689	1.258
27692	hsa-miR-886-3p	-1.223
17878	hsa-miR-193a-5p	1.094
17413	hsa-miR-565	-1.375
11124	hsa-miR-492	1.210
17559	mmu-miR-715	0.983
17280	hsa-miR-15b	-0.995
29872	hsa-miR-340	-0.683
13137	hsa-miR-518e*/519a*/519b-5p/519c-5p/522*/523*	1.111
11023	hsa-miR-222	-0.539
11065	hsa-miR-335	1.300
27720	hsa-miR-15a	-0.691
17512	mmu-miR-711	0.538
28232	miRPlus_28232	0.736
4890	hsa-miR-19b	-0.587
10967	hsa-miR-16	-0.866
11048	hsa-miR-30a	0.577
17950	hsa-miR-371-5p	0.851
17894	hsa-miR-501-3p	0.593
19580	hsa-let-7i	-0.557
28736	hsa-miR-17	-0.473
11020	hsa-miR-22	0.445
11039	hsa-miR-29a	0.450
10986	hsa-miR-193a-3p	-0.484
17309	hsa-miR-623	0.722
27560	miRPlus_27560	0.665
11089	hsa-miR-376a	-0.471
17903	hsa-miR-940	0.465
28950	hsa-miR-455-3p	-0.475
27217	hsa-miR-34a	0.539
11125	hsa-miR-493*	-0.502
10964	hsa-miR-155	-0.558
17510	hsa-miR-602	0.979
10999	hsa-miR-20a	-0.487
19594	hsa-miR-296-5p	0.526
11030	hsa-miR-26a	0.397

Fold Change	log2 Average Intensity	p-value	FDR adjusted p-value
7.390	10.413	4.43E-20	3.57E-17
9.537	10.551	9.03E-19	3.64E-16
5.899	9.984	2.89E-18	7.76E-16
6.039	10.390	9.74E-17	1.96E-14
6.894	8.850	2.21E-16	3.56E-14
2.971	8.920	2.22E-14	2.99E-12
2.842	9.083	7.37E-14	8.49E-12
3.436	10.007	1.53E-13	1.54E-11
2.044	13.715	1.93E-12	1.73E-10
2.101	8.453	2.75E-12	2.22E-10
3.401	9.007	1.40E-11	1.03E-09
2.440	8.676	2.89E-11	1.94E-09
-2.357	9.159	5.46E-11	3.37E-09
3.422	9.065	5.86E-11	3.37E-09
-2.252	9.878	9.71E-11	5.22E-09
2.392	8.434	1.38E-10	6.93E-09
-2.334	10.984	1.66E-10	7.87E-09
2.134	9.401	1.53E-09	6.87E-08
-2.594	8.397	1.32E-08	5.62E-07
2.314	8.460	1.40E-08	5.65E-07
1.976	8.118	3.18E-08	1.22E-06
-1.993	8.817	3.36E-08	1.23E-06
-1.605	9.382	1.38E-07	4.82E-06
2.160	8.022	5.76E-07	1.93E-05
-1.453	11.388	1.97E-06	6.34E-05
2.462	7.188	2.46E-06	7.63E-05
-1.614	9.378	4.22E-06	1.26E-04
1.452	10.904	7.89E-06	2.27E-04
1.666	7.941	1.44E-05	3.99E-04
-1.502	9.245	1.50E-05	4.04E-04
-1.822	9.227	1.64E-05	4.26E-04
1.492	10.047	5.01E-05	1.26E-03
1.804	7.780	6.16E-05	1.51E-03
1.508	8.094	1.14E-04	2.70E-03
-1.472	10.503	2.57E-04	5.92E-03
-1.388	8.332	4.74E-04	1.06E-02
1.362	11.931	6.73E-04	1.47E-02
1.366	12.606	7.11E-04	1.51E-02
-1.399	10.900	8.44E-04	1.74E-02
1.650	7.453	9.68E-04	1.94E-02
1.586	7.814	9.89E-04	1.94E-02
-1.386	8.536	1.01E-03	1.94E-02
1.380	7.935	1.23E-03	2.30E-02
-1.390	7.998	1.25E-03	2.30E-02
1.453	10.333	1.41E-03	2.52E-02
-1.416	8.060	1.61E-03	2.82E-02
-1.472	7.321	1.69E-03	2.85E-02
1.971	7.938	1.70E-03	2.85E-02
-1.401	7.740	2.14E-03	3.52E-02
1.440	8.021	2.76E-03	4.39E-02
1.317	10.869	2.78E-03	4.39E-02

Exiqon Reporter ID (v9.2)	Reporter Name	log2 Fold Change	Fold Change	log2 Average Intensity
27565	hsa-miR-423-5p	0.695	1.619	13.224
4890	hsa-miR-19b	-0.835	-1.784	11.347
28736	hsa-miR-17	-0.787	-1.725	11.359
28737	hsa-miR-106a	-0.658	-1.578	10.987
19581	hsa-miR-100	0.551	1.465	12.008
17521	mmu-miR-714	0.493	1.407	10.837
17869	miRPlus_17869	-0.444	-1.361	11.852
17583	mmu-miR-720	-0.393	-1.313	13.263
17321	mmu-miR-689	0.368	1.291	11.361
19599	mmu-miR-106a	-0.611	-1.527	10.110
27898	hsa-miR-768-3p	0.621	1.538	11.138
11078	hsa-miR-365	0.608	1.524	10.939
10967	hsa-miR-16	-0.645	-1.564	10.209
30787	hsa-miR-125b	0.522	1.436	11.641
32883	hsa-miR-801	-0.466	-1.381	11.055
17952	miRPlus_17952	-0.334	-1.260	12.096
27692	hsa-miR-886-3p	-0.427	-1.345	13.130
10999	hsa-miR-20a	-0.539	-1.453	10.644

p-value	FDR adjusted p-value
4.41E-08	3.55E-05
2.93E-07	1.18E-04
7.55E-07	1.85E-04
9.42E-06	1.30E-03
9.67E-06	1.30E-03
3.40E-05	3.91E-03
5.30E-05	5.34E-03
1.86E-04	1.56E-02
2.01E-04	1.56E-02
2.14E-04	1.56E-02
2.64E-04	1.77E-02
3.53E-04	2.19E-02
3.81E-04	2.19E-02
7.03E-04	3.78E-02
9.38E-04	4.73E-02
1.02E-03	4.75E-02
1.10E-03	4.75E-02
1.12E-03	4.75E-02

Exiqon Reporter ID (v8.0)	Reporter Name	log2 Fold Change	Fold Change
10306	hsa-miR-146b	1.961	3.893
10986	hsa-miR-193a	-1.014	-2.019
11030	hsa-miR-26a	0.902	1.868
10924	hsa-miR-10a	0.894	1.858
10952	hsa-miR-146a	2.099	4.285
11062	hsa-miR-33	-0.897	-1.863
11050	hsa-miR-30c	0.632	1.549
11051	hsa-miR-30d	0.835	1.784
11048	hsa-miR-30a-5p	0.708	1.634
10925	hsa-miR-10b	1.005	2.007
10997	hsa-miR-19a	-0.791	-1.730
13173	hsa-miR-17	-0.903	-1.870
11006	hsa-miR-205	-2.216	-4.647
10977	hsa-miR-183	-0.555	-1.469
11031	hsa-miR-26b	0.762	1.695
10968	hsa-miR-17*	-0.586	-1.501
10967	hsa-miR-16	-0.665	-1.586
10918	hsa-miR-101	0.549	1.463
10966	hsa-miR-15b	-0.708	-1.634
11260	rno-miR-151*	0.638	1.556
11216	mmu-miR-292-5p	-0.392	-1.312
11258	rno-miR-140*	0.727	1.655
11224	hsa-miR-30e-3p	0.651	1.570
11009	hsa-miR-20b	-0.738	-1.667
10998	hsa-miR-19b	-0.698	-1.623
11203	hsa-miR-155_MM1	-0.552	-1.466
11196	hsa-miR-30c_MM2	0.550	1.464
11047	hsa-miR-30a-3p	0.505	1.419
5560	hsa-miR-185	-0.390	-1.310
11200	mmu-miR-129-3p	0.833	1.782
11004	hsa-miR-203	-0.455	-1.371
10990	hsa-miR-196a	-0.453	-1.369
11183	hsa-miR-99a	0.951	1.933
13131	hsa-miR-518c*	-0.447	-1.363
3320	hsa-let-7a	0.631	1.548
11020	hsa-miR-22	0.506	1.420
11039	hsa-miR-29a	0.470	1.385
10913	hsa-let-7c	0.629	1.546
11067	hsa-miR-338	0.424	1.341
11182	hsa-miR-98	0.338	1.264
10978	hsa-miR-184	-0.371	-1.293
11186	hsa-let-7a_MM2	0.513	1.427
11273	rno-miR-352	0.437	1.354
10938	hsa-miR-133a-133b	0.586	1.501
11199	hsa-miR-106b_MM2	-0.448	-1.365
11064	hsa-miR-331	0.413	1.332
11184	hsa-miR-99b	0.583	1.498
11245	mmu-miR-433-5p	-0.357	-1.281
10971	hsa-miR-181a	0.478	1.393
11072	hsa-miR-34a	0.898	1.864
10999	hsa-miR-20a	-0.534	-1.448

11034	hsa-miR-28	0.393	1.313
11002	hsa-miR-200c	-0.281	-1.215
11214	mmu-miR-291a-5p	-0.378	-1.300
13174	hsa-miR-30e-5p	0.421	1.339
11107	hsa-miR-424	-0.286	-1.220
13150	hsa-miR-424_MM1	-0.313	-1.242
13169	mmu-let-7d*	-0.425	-1.343
4500	hsa-let-7g	0.306	1.237
10972	hsa-miR-181b	0.303	1.234
10921	hsa-miR-106a	-0.431	-1.348
13141	hsa-miR-18b	-0.389	-1.309
10965	hsa-miR-15a	-0.323	-1.251
10912	hsa-let-7b	0.237	1.178
10586	hsa-miR-518f*-526a	-0.221	-1.165
11175	hsa-miR-525	-0.257	-1.195
10985	hsa-miR-191	0.371	1.293
11235	mmu-miR-351	-0.281	-1.215
10935	hsa-miR-130a	0.256	1.194
11176	hsa-miR-526b	-0.264	-1.201
10964	hsa-miR-155	-0.308	-1.238

log2 Average Intensity	p-value	FDR adjusted p-value
8.861	3.81E-17	1.71E-14
11.655	4.72E-15	1.06E-12
10.899	9.34E-14	1.40E-11
11.393	1.53E-13	1.71E-11
8.710	2.86E-12	2.57E-10
9.852	3.46E-12	2.59E-10
12.153	4.72E-12	3.03E-10
9.984	7.00E-12	3.93E-10
11.885	2.88E-11	1.43E-09
11.358	7.74E-11	3.16E-09
9.090	1.40E-10	5.22E-09
9.399	2.31E-10	7.97E-09
9.096	2.49E-10	7.97E-09
11.644	1.12E-09	3.35E-08
10.386	1.96E-09	5.51E-08
8.229	1.10E-08	2.90E-07
10.359	2.58E-08	6.45E-07
9.727	1.09E-07	2.58E-06
10.384	2.48E-07	5.56E-06
9.151	3.39E-07	7.24E-06
13.213	1.65E-06	3.36E-05
8.728	2.43E-06	4.74E-05
9.788	2.68E-06	5.01E-05
8.188	4.55E-06	8.18E-05
9.271	7.96E-06	1.37E-04
9.999	1.02E-05	1.63E-04
11.335	1.00E-05	1.63E-04
9.236	1.19E-05	1.84E-04
12.642	1.23E-05	1.84E-04
8.220	1.65E-05	2.39E-04
9.045	1.87E-05	2.62E-04
8.516	2.59E-05	3.53E-04
7.730	2.98E-05	3.94E-04
11.401	3.28E-05	4.21E-04
13.860	4.28E-05	5.34E-04
10.797	4.50E-05	5.46E-04
13.071	6.30E-05	7.45E-04
13.407	8.35E-05	9.49E-04
8.547	8.67E-05	9.49E-04
11.633	8.66E-05	9.49E-04
11.554	1.15E-04	1.22E-03
9.730	1.56E-04	1.63E-03
10.554	1.99E-04	2.03E-03
8.713	2.04E-04	2.04E-03
8.734	2.30E-04	2.19E-03
9.594	2.29E-04	2.19E-03
8.762	2.55E-04	2.39E-03
12.882	3.44E-04	3.15E-03
8.541	3.97E-04	3.57E-03
9.321	4.48E-04	3.94E-03
9.080	5.37E-04	4.60E-03

8.711	5.43E-04	4.60E-03
10.953	9.38E-04	7.78E-03
8.862	9.53E-04	7.78E-03
9.632	9.80E-04	7.86E-03
10.217	1.07E-03	8.30E-03
10.310	1.06E-03	8.30E-03
10.745	1.14E-03	8.54E-03
12.233	1.28E-03	9.43E-03
9.306	1.46E-03	1.06E-02
9.015	1.73E-03	1.22E-02
8.597	1.74E-03	1.22E-02
9.488	1.84E-03	1.27E-02
13.329	1.87E-03	1.27E-02
12.167	3.23E-03	2.17E-02
13.182	4.17E-03	2.75E-02
9.016	4.27E-03	2.78E-02
13.929	6.00E-03	3.85E-02
9.843	6.28E-03	3.97E-02
11.352	6.47E-03	4.04E-02
10.420	7.11E-03	4.38E-02

Exiqon Reporter ID (v9.2)	Reporter Name	log2 Fold Change	Fold Change	log2 Average Intensity
5740	hsa-miR-21	1.197	2.436	12.155
32789	hsa-miR-92a	-1.447	-2.797	9.553
28399	hsa-miR-23a	1.075	2.121	12.859
11027	hsa-miR-23b	0.988	2.006	12.246
11020	hsa-miR-22	1.163	2.364	10.710
4890	hsa-miR-19b	-1.030	-2.081	12.623
11030	hsa-miR-26a	-0.541	-0.992	13.658
17558	hsa-miR-663	1.432	2.908	8.670
17890	miRPlus_17890	0.855	1.836	10.328
11040	hsa-miR-29b	-0.507	-0.961	12.293
11041	hsa-miR-29c	-0.686	-1.630	11.262
21472	miRPlus_21472	0.888	1.866	10.766
17565	hsa-miR-30b	-0.718	-1.666	12.390
29204	hsa-miR-378	-0.992	-2.011	8.626
19593	hsa-miR-27a	0.907	1.879	11.276
19596	hsa-miR-30d	-0.917	-1.908	10.816
17506	hsa-miR-24	0.716	1.649	11.115
27565	hsa-miR-423-5p	-0.756	-1.694	11.140
10306	hsa-miR-146b-5p	-0.851	-1.808	11.572
11065	hsa-miR-335	-1.504	-2.911	9.417
17502	hsa-miR-30c	-0.647	-1.579	12.003
17718	hsa-miR-92b	-0.732	-1.671	8.762
17865	miRPlus_17865	-0.971	-1.991	9.689
19602	hsa-let-7g	-0.677	-1.601	11.325
31026	hsa-miR-101	-0.668	-1.174	12.043
11052	hsa-miR-31	-1.123	-2.191	9.191
11048	hsa-miR-30a	-0.602	-1.525	11.382
10999	hsa-miR-20a	-1.168	-2.283	10.490
27533	hsa-miR-320	-1.277	-2.455	9.922
28737	hsa-miR-106a	-0.913	-1.887	10.385
11106	hsa-miR-423-3p	-0.620	-1.545	9.626
19594	hsa-miR-296-5p	0.747	1.708	9.032
28736	hsa-miR-17	-0.697	-1.628	10.821
10971	hsa-miR-181a	-0.615	-1.551	9.342
27544	hsa-miR-363*	-0.857	-1.829	9.495
11053	hsa-miR-32	1.015	2.045	9.228

p-value	FDR adjusted p-value
2.09E-18	1.68E-15
5.84E-18	2.35E-15
1.64E-15	4.41E-13
4.87E-14	9.82E-12
5.22E-12	7.01E-10
4.72E-11	5.44E-09
8.15E-11	8.21E-09
5.89E-10	5.27E-08
7.06E-10	5.69E-08
8.82E-09	5.27E-07
3.54E-08	1.78E-06
9.30E-08	4.41E-06
1.19E-07	5.04E-06
2.05E-07	8.26E-06
2.68E-07	1.03E-05
3.50E-07	1.28E-05
6.68E-07	2.24E-05
1.45E-06	4.69E-05
1.72E-06	5.35E-05
3.07E-06	9.17E-05
4.03E-06	1.16E-04
1.11E-05	2.72E-04
1.09E-05	2.72E-04
1.71E-05	3.95E-04
1.72E-05	3.95E-04
1.84E-05	4.12E-04
1.97E-05	4.19E-04
2.65E-05	5.35E-04
3.99E-05	7.85E-04
3.12E-04	5.84E-03
3.55E-04	6.26E-03
4.07E-04	6.98E-03
4.93E-04	8.28E-03
1.36E-03	2.07E-02
3.24E-03	4.49E-02
3.48E-03	4.67E-02

Exiqon Reporter ID (v9.2)	Reporter Name	log2 Fold Change	Fold Change	log2 Average Intensity
11163	hsa-miR-519d	-0.855	-1.808	10.856
10997	hsa-miR-19a	-0.755	-1.687	10.615
4890	hsa-miR-19b	-0.475	-1.390	9.649
11107	hsa-miR-424	-0.472	-1.387	9.598
19592	hsa-miR-212	-0.428	-1.345	10.564
17748	hsa-let-7a	-0.356	-1.280	10.874
10999	hsa-miR-20a	-0.574	-1.488	8.688
17280	hsa-miR-15b	-0.637	-1.555	9.190
27217	hsa-miR-34a	0.448	1.364	9.430
10987	hsa-miR-193b	-0.365	-1.288	9.906
28736	hsa-miR-17	-0.619	-1.536	9.032
14293	mmu-miR-546	-0.300	-1.231	10.283
10967	hsa-miR-16	-0.446	-1.362	9.361
21472	miRPlus_21472	0.295	1.227	11.536
11182	hsa-miR-98	-0.374	-1.296	8.903
10914	mmu-let-7d	-0.315	-1.244	11.671
13150	mmu-miR-322	-0.618	-1.535	8.274
11201	miRPlus_11201	-0.404	-1.323	9.138
11027	hsa-miR-23b	-0.224	-1.168	11.619

p-value	FDR adjusted p-value
1.49E-10	1.20E-07
8.09E-07	3.26E-04
9.11E-05	2.45E-02
3.33E-04	5.26E-02
3.35E-04	5.26E-02
4.34E-04	5.26E-02
4.57E-04	5.26E-02
8.50E-04	8.56E-02
9.59E-04	8.59E-02
1.95E-03	1.46E-01
2.00E-03	1.46E-01
2.29E-03	1.46E-01
2.35E-03	1.46E-01
3.74E-03	2.16E-01
4.86E-03	2.61E-01
5.20E-03	2.62E-01
6.14E-03	2.91E-01
7.08E-03	3.17E-01
8.12E-03	3.45E-01

Exiqon Reporter ID (v9.2)	Reporter Name	log2 Fold Change
11027	hsa-miR-144	2.293
11006	hsa-miR-100	-0.975
11235	hsa-miR-99a	-0.997
5740	hsa-miR-199b-5p	-1.403
11039	hsa-miR-338-3p	-1.384
28232	hsa-miR-451	1.077
11135	hsa-miR-10a	-1.066
17832	hsa-miR-519e*	0.917
27554	hsa-miR-335	-1.223
13175	hsa-miR-492	0.879
11020	hsa-miR-125b	-0.524
10946	hsa-miR-30d	-0.754
11130	hsa-miR-26a	-0.463
14287	hsa-miR-130a	-0.851
11175	hsa-miR-181a	-0.755
11040	hsa-miR-30c	-0.817
21757	hsa-miR-326	-0.574
13180	miRPlus_17925	0.912
19593	miRPlus_17952	1.337
4890	mmu-miR-199b*	-0.517
19594	mmu-miR-711	0.741
11048	hsa-miR-583	1.039
11030	mmu-miR-351	0.976
31026	mmu-miR-714	1.174
13137	hsa-miR-28-5p	-0.691
17915	miRPlus_17945	-0.587
11229	miRPlus_17848	-0.972
4610	hsa-miR-565	-0.933
10934	hsa-miR-184	0.605
17510	hsa-miR-886-3p	-1.079
11246	hsa-let-7d	-0.430
27566	hsa-let-7g	-0.576
30317	hsa-miR-183*	0.868
28431	mmu-miR-300	0.739
	hsa-miR-489	-0.510
	hsa-miR-152	-0.624
	hsa-miR-658	0.728
	hsa-miR-374b	-0.688
	hsa-miR-584	0.495
	hsa-miR-191	-0.698
	hsa-miR-30e	-0.581
	hsa-miR-30b*	0.674
	hsa-miR-199a-3p/199b-3p	-0.734
	hsa-miR-376a	-0.542
	miRPlus_28575	0.610
	hsa-miR-200c	-0.634
	hsa-miR-30b	-0.811
	hsa-miR-525-5p	1.018
	hsa-let-7f	-0.610
	hsa-miR-486-5p	0.787
	hsa-miR-602	0.476

hsa-miR-96*	0.700
hsa-miR-642	-0.465
hsa-miR-199a-5p	-0.443
hsa-miR-342-3p	-0.656
miRPlus_27564	0.998
mmu-miR-374	-0.614
hsa-miR-148b	-0.552
hsa-miR-199a-3p/199b-3p	-0.737
hsa-let-7a	-0.657
hsa-miR-196a	-0.749
hsa-miR-30e*	-0.755
hsa-miR-483-5p	0.942
hsa-miR-99b	-0.420
hsa-miR-765	1.119
hsa-miR-10b	-0.777
hsa-miR-214	-0.456
hsa-miR-29a	0.383
hsa-miR-381	0.590
hsa-miR-374a	-0.647
hsa-miR-675	0.757
hsa-miR-149	-0.614
hsa-miR-126*	-0.562
hsa-miR-424	-0.718
mmu-miR-322	-0.755
hsa-miR-107	-0.508
hsa-miR-518d-5p/518f*/520c-5p/526a	0.500
mmu-miR-291b-5p	0.515
hsa-miR-526b	0.587
mmu-miR-320	0.461
mmu-miR-710	0.752
hsa-let-7i	-0.299
hsa-miR-101	-0.506
hsa-miR-512-5p	0.334
mmu-let-7a	-0.666
hsa-miR-151-5p	-0.449
hsa-miR-671-5p	0.545
hsa-miR-126	-0.580
hsa-miR-361-5p	-0.413
mmu-miR-330*	0.408
hsa-miR-154*	0.746
hsa-miR-518c*	0.637
hsa-miR-198	0.801
hsa-miR-518a-5p/527	0.470
hsa-miR-15b	-0.477
hsa-miR-423-3p	0.420
mmu-miR-666-5p	0.529
hsa-miR-432*	0.455
hsa-miR-494	0.322
hsa-miR-543	0.492
hsa-miR-98	-0.302
hsa-miR-19a	-0.407
hsa-miR-210	-0.356

miRPlus_17921	0.533
miRPlus_17930	0.317
hsa-miR-744	-0.491
hsa-miR-768-5p	-0.664
hsa-miR-320	-0.427
hsa-miR-203	-0.444
hsa-miR-376b	-0.454
hsa-miR-200b	-0.391
mmu-miR-690	-0.476
miRPlus_17957	-0.584
hsa-miR-125a-5p	-0.284
hsa-miR-221	-0.446
hsa-miR-371-5p	0.382
hsa-miR-185	0.587
hsa-miR-127-3p	-0.520
mmu-let-7d	-0.378
mmu-miR-720	0.285
mmu-miR-691	0.428
hsa-miR-212	-0.380
hsa-miR-518e*/519a*/519b-5p/519c-5p/522*/523*	0.536
hsa-miR-146b-5p	-0.417
hsa-miR-425*	0.463
mmu-miR-708	-0.476
mmu-miR-709	0.444
hsa-miR-328	-0.331
hsa-miR-196b	-0.485
mmu-miR-380-3p	0.584
miRPlus_17865	-0.357
hsa-miR-369-3p	0.919
hsa-miR-886-5p	-0.386
hsa-miR-21	0.417
hsa-miR-205	-0.365
hsa-miR-186	-0.440
hsa-miR-365	-0.365
mmu-miR-667	-0.305
mmu-miR-429	-0.418
hsa-miR-222	-0.317
mmu-miR-718	0.393
hsa-miR-15a	-0.357
hsa-miR-557	0.404
hsa-miR-625	0.421
mmu-miR-434-3p	0.507
hsa-miR-31	0.723
hsa-miR-429	-0.411
hsa-miR-604	0.471
hsa-miR-490-3p	0.406
hsa-miR-92b	-0.356
mmu-miR-298	0.749
hsa-miR-151-3p	-0.373
hsa-miR-20a	-0.453
hsa-miR-218	-0.686
miRPlus_17833	-0.369

hsa-miR-498	0.406
hsa-miR-302c*	0.267
hsa-miR-572	-0.330
hsa-let-7a*	-0.406
hsa-miR-22	-0.341
miRPlus_17890	0.301
mmu-miR-106a	-0.350
hsa-miR-17	-0.475
hsa-miR-20b	-0.456
hsa-miR-516b	0.451
miRPlus_28232	-0.289
mmu-miR-298	0.691
hsa-miR-768-3p	-0.217
hsa-miR-379	-0.420
hsa-miR-801	0.363
miRPlus_30317	-0.442
hsa-miR-24	-0.192
hsa-miR-27b	-0.237
miRPlus_21472	0.304
hsa-miR-566	0.326
hsa-let-7b	-0.193
hsa-miR-103	-0.263
mmu-miR-693-5p	-0.421
hsa-miR-376c	-0.409
hsa-miR-142-5p	0.419
hsa-miR-146a	-0.316
hsa-miR-663	0.337
hsa-miR-193b	-0.326
mmu-miR-712	0.287
mmu-miR-669a	-0.283
hsa-miR-181b	-0.345
mmu-miR-34b-5p	0.491
mmu-miR-712*	0.502
hsa-miR-106a	-0.355
hsa-miR-141	-0.327

Fold Change	log2 Average Intensity	p-value	FDR adjusted p-value
4.902	10.847	7.8E-29	6.3E-26
-1.966	10.689	3.2E-19	1.3E-16
-1.996	10.423	1.1E-18	2.9E-16
-2.645	10.490	7.9E-18	1.5E-15
-2.609	9.671	9.1E-18	1.5E-15
2.110	11.897	4.4E-16	5.9E-14
-2.093	10.073	2.3E-15	2.6E-13
1.888	11.515	3.9E-14	3.9E-12
-2.334	8.619	1.7E-13	1.6E-11
1.839	12.380	2.3E-12	1.9E-10
-1.438	12.802	1.8E-11	1.2E-09
-1.687	11.365	1.7E-11	1.2E-09
-1.379	13.306	1.3E-10	7.8E-09
-1.804	10.132	1.8E-10	1.0E-08
-1.687	9.262	2.0E-10	1.0E-08
-1.762	11.496	2.0E-10	1.0E-08
-1.488	11.620	2.8E-10	1.3E-08
1.881	10.088	4.1E-10	1.8E-08
2.527	12.307	4.6E-10	2.0E-08
-1.431	11.189	7.2E-10	2.9E-08
1.671	13.790	8.1E-10	3.1E-08
2.054	10.859	1.1E-09	4.0E-08
1.967	12.863	2.3E-09	8.2E-08
2.257	11.763	2.5E-09	8.5E-08
-1.615	8.836	3.3E-09	1.1E-07
-1.502	9.090	4.3E-09	1.3E-07
-1.962	10.014	9.1E-09	2.7E-07
-1.909	9.665	9.9E-09	2.8E-07
1.521	10.650	1.2E-08	3.1E-07
-2.112	10.789	1.1E-08	3.1E-07
-1.347	12.441	1.2E-08	3.1E-07
-1.490	10.093	1.4E-08	3.5E-07
1.825	11.019	2.7E-08	6.7E-07
1.669	9.768	3.1E-08	7.3E-07
-1.424	10.081	5.8E-08	1.3E-06
-1.541	9.012	9.9E-08	2.2E-06
1.657	10.958	1.2E-07	2.5E-06
-1.611	9.547	1.3E-07	2.7E-06
1.409	9.802	1.4E-07	2.9E-06
-1.622	10.151	1.6E-07	3.2E-06
-1.496	11.264	2.6E-07	5.1E-06
1.595	12.251	4.2E-07	8.1E-06
-1.663	11.418	4.7E-07	8.9E-06
-1.456	8.928	5.2E-07	9.4E-06
1.526	9.912	5.1E-07	9.4E-06
-1.552	11.675	5.8E-07	1.0E-05
-1.755	11.274	5.7E-07	1.0E-05
2.025	12.258	6.3E-07	1.1E-05
-1.526	11.505	7.9E-07	1.3E-05
1.725	8.518	8.0E-07	1.3E-05
1.390	11.593	9.4E-07	1.5E-05

1.624	9.878	9.8E-07	1.5E-05
-1.380	10.015	1.0E-06	1.6E-05
-1.360	11.294	1.3E-06	1.9E-05
-1.576	8.910	1.3E-06	1.9E-05
1.998	10.797	1.4E-06	2.0E-05
-1.531	10.425	1.5E-06	2.1E-05
-1.467	9.605	1.6E-06	2.2E-05
-1.667	11.356	1.6E-06	2.2E-05
-1.577	13.106	1.7E-06	2.3E-05
-1.681	8.436	1.8E-06	2.4E-05
-1.688	8.702	1.8E-06	2.4E-05
1.922	11.168	1.9E-06	2.4E-05
-1.338	10.628	1.9E-06	2.4E-05
2.172	12.523	2.6E-06	3.2E-05
-1.714	9.123	2.7E-06	3.3E-05
-1.372	10.125	3.6E-06	4.3E-05
1.304	13.115	5.3E-06	6.2E-05
1.505	10.970	5.3E-06	6.2E-05
-1.566	9.543	6.1E-06	7.1E-05
1.690	8.627	7.1E-06	8.0E-05
-1.530	8.005	8.0E-06	9.0E-05
-1.476	9.979	8.2E-06	9.1E-05
-1.645	8.640	9.6E-06	1.0E-04
-1.688	8.651	9.8E-06	1.1E-04
-1.422	10.441	1.1E-05	1.1E-04
1.414	9.952	1.1E-05	1.2E-04
1.429	10.460	1.3E-05	1.3E-04
1.502	9.475	1.3E-05	1.4E-04
1.376	11.784	1.4E-05	1.4E-04
1.685	9.315	1.4E-05	1.4E-04
-1.230	12.071	2.1E-05	2.1E-04
-1.421	12.040	2.2E-05	2.1E-04
1.260	10.959	2.4E-05	2.3E-04
-1.587	13.021	2.8E-05	2.6E-04
-1.366	8.854	2.8E-05	2.6E-04
1.459	11.444	2.9E-05	2.6E-04
-1.494	12.039	2.9E-05	2.6E-04
-1.332	9.661	3.1E-05	2.8E-04
1.327	9.949	3.2E-05	2.9E-04
1.677	9.759	3.4E-05	3.0E-04
1.555	10.871	3.9E-05	3.4E-04
1.743	10.856	4.5E-05	3.9E-04
1.386	11.330	4.8E-05	4.1E-04
-1.392	10.405	4.9E-05	4.1E-04
1.338	11.481	5.3E-05	4.4E-04
1.443	9.688	6.0E-05	4.9E-04
1.371	9.046	7.1E-05	5.8E-04
1.250	13.078	9.1E-05	7.4E-04
1.407	8.895	9.2E-05	7.4E-04
-1.233	12.273	9.1E-05	7.4E-04
-1.326	12.950	9.5E-05	7.5E-04
-1.279	11.523	9.8E-05	7.6E-04

1.447	10.401	9.7E-05	7.6E-04
1.245	11.471	1.2E-04	9.4E-04
-1.406	7.914	1.3E-04	9.9E-04
-1.585	9.619	1.3E-04	1.0E-03
-1.344	10.560	1.4E-04	1.0E-03
-1.360	12.748	1.7E-04	1.2E-03
-1.370	8.389	1.7E-04	1.2E-03
-1.312	11.718	1.8E-04	1.3E-03
-1.391	9.716	1.8E-04	1.3E-03
-1.499	8.768	1.9E-04	1.4E-03
-1.217	11.964	2.1E-04	1.5E-03
-1.362	11.180	2.4E-04	1.7E-03
1.303	11.098	2.7E-04	1.9E-03
1.502	11.354	2.9E-04	2.0E-03
-1.433	9.540	3.0E-04	2.0E-03
-1.300	13.016	3.0E-04	2.1E-03
1.219	11.093	3.1E-04	2.1E-03
1.345	10.493	3.2E-04	2.2E-03
-1.301	14.192	4.0E-04	2.6E-03
1.450	11.063	4.0E-04	2.6E-03
-1.335	10.249	4.2E-04	2.7E-03
1.378	8.624	4.6E-04	3.0E-03
-1.390	8.186	4.7E-04	3.0E-03
1.360	10.792	4.8E-04	3.0E-03
-1.258	8.819	4.9E-04	3.1E-03
-1.399	8.190	5.0E-04	3.2E-03
1.499	9.094	5.2E-04	3.2E-03
-1.281	10.479	5.6E-04	3.4E-03
1.890	12.179	6.0E-04	3.6E-03
-1.307	9.126	6.0E-04	3.6E-03
1.335	13.766	6.4E-04	3.9E-03
-1.288	13.849	7.0E-04	4.2E-03
-1.357	8.646	7.6E-04	4.5E-03
-1.288	10.401	8.2E-04	4.8E-03
-1.235	11.697	8.5E-04	5.0E-03
-1.336	8.463	8.8E-04	5.1E-03
-1.246	11.230	9.2E-04	5.3E-03
1.313	8.893	9.5E-04	5.4E-03
-1.281	11.130	9.7E-04	5.5E-03
1.323	11.813	9.8E-04	5.5E-03
1.339	8.629	1.1E-03	5.9E-03
1.421	9.261	1.1E-03	6.3E-03
1.651	7.801	1.2E-03	6.5E-03
-1.330	8.740	1.2E-03	6.7E-03
1.386	8.780	1.2E-03	6.7E-03
1.325	8.421	1.3E-03	7.1E-03
-1.280	9.186	1.4E-03	7.5E-03
1.680	10.267	1.5E-03	7.9E-03
-1.295	8.760	1.5E-03	8.0E-03
-1.369	10.470	1.6E-03	8.3E-03
-1.609	7.730	1.7E-03	8.7E-03
-1.292	8.996	1.8E-03	9.5E-03

1.325	12.603	1.9E-03	9.6E-03
1.203	10.873	1.9E-03	9.9E-03
-1.257	9.504	2.0E-03	1.0E-02
-1.325	8.237	2.1E-03	1.1E-02
-1.266	12.120	2.2E-03	1.1E-02
1.232	12.425	2.2E-03	1.1E-02
-1.275	10.123	2.2E-03	1.1E-02
-1.390	10.702	2.6E-03	1.3E-02
-1.372	8.890	2.6E-03	1.3E-02
1.367	10.746	2.6E-03	1.3E-02
-1.222	11.192	2.6E-03	1.3E-02
1.615	10.262	2.8E-03	1.4E-02
-1.163	12.121	2.9E-03	1.4E-02
-1.338	8.907	2.9E-03	1.4E-02
1.286	10.346	3.0E-03	1.4E-02
-1.358	8.387	3.7E-03	1.8E-02
-1.142	13.110	3.9E-03	1.8E-02
-1.178	13.211	4.0E-03	1.9E-02
1.234	13.439	4.2E-03	1.9E-02
1.254	8.620	4.5E-03	2.1E-02
-1.143	12.762	5.0E-03	2.3E-02
-1.200	10.530	5.1E-03	2.3E-02
-1.339	8.387	5.3E-03	2.4E-02
-1.328	8.233	5.4E-03	2.4E-02
1.337	9.378	5.7E-03	2.6E-02
-1.245	9.577	6.3E-03	2.8E-02
1.263	10.002	6.4E-03	2.8E-02
-1.254	9.716	6.5E-03	2.9E-02
1.220	8.302	6.8E-03	3.0E-02
-1.216	8.800	7.6E-03	3.3E-02
-1.270	7.970	9.1E-03	3.9E-02
1.406	7.458	9.2E-03	4.0E-02
1.416	7.910	1.0E-02	4.3E-02
-1.279	10.647	1.1E-02	4.5E-02
-1.254	11.604	1.2E-02	4.9E-02

Exiqon Reporter ID (v9.2)	Reporter Name	log2 Fold Change	Fold Change	log2 Average Intensity
5740	hsa-miR-21	-2.608	-6.097	12.155
4890	hsa-miR-19b	-1.456	-2.743	12.623
28399	hsa-miR-23a	1.246	2.372	12.859
27898	hsa-miR-768-3p	0.863	1.819	14.583
11163	hsa-miR-519d	-1.380	-2.603	11.392
28736	hsa-miR-17	-1.438	-2.710	10.821
11040	hsa-miR-29b	-1.226	-2.339	12.293
29871	hsa-miR-768-5p	0.817	1.762	13.086
27720	hsa-miR-15a	-2.185	-4.548	10.242
21753	hsa-miR-668	1.813	3.514	13.741
13174	hsa-miR-30e	-1.934	-3.821	10.910
14285	hsa-miR-487b	-1.272	-2.414	9.796
19592	hsa-miR-212	-1.558	-2.945	10.735
19593	hsa-miR-27a	-0.936	-1.913	11.276
17752	hsa-let-7f	-1.538	-2.904	9.555
32884	hsa-miR-342-3p	0.655	1.575	12.671
19580	hsa-let-7i	-0.912	-1.882	10.855
11175	hsa-miR-525-5p	-1.373	-2.589	9.014
10997	hsa-miR-19a	-0.972	-1.961	11.892
17927	hsa-miR-491-3p	-0.887	-1.849	10.146
11027	hsa-miR-23b	0.409	1.328	12.246
11041	hsa-miR-29c	-0.505	-1.419	11.262
29872	hsa-miR-340	-0.906	-1.874	9.510
10928	hsa-miR-125a-5p	-0.948	-1.929	9.602
11065	hsa-miR-335	-1.249	-2.377	9.417
31809	hsa-miR-590-5p	-1.178	-2.263	8.869
11009	hsa-miR-20b	-1.098	-2.141	9.220
10306	hsa-miR-146b-5p	0.672	1.594	11.572
13175	hsa-miR-27b	-0.551	-1.465	10.898
11130	hsa-miR-498	-0.508	-1.422	9.630
19582	hsa-miR-106b	-0.747	-1.678	10.368
11182	hsa-miR-98	-0.831	-1.778	9.027
19004	hsa-let-7c	0.418	1.336	10.890
32883	hsa-miR-801	-0.457	-1.373	10.162
17280	hsa-miR-15b	-0.502	-1.417	11.281
13141	hsa-miR-18b	-0.721	-1.648	9.298
11007	hsa-miR-206	-0.928	-1.902	8.695
31026	hsa-miR-101	-0.986	-1.981	12.043
10964	hsa-miR-155	-0.730	-1.659	9.886
17869	miRPlus_17869	-0.450	-1.366	10.059
11022	hsa-miR-221	-0.702	-1.626	9.654
18739	hsa-miR-186	-0.804	-1.746	9.433
14287	hsa-miR-494	-0.790	-1.729	8.964
10952	hsa-miR-146a	-0.476	-1.391	10.377
11015	hsa-miR-215	-0.471	-1.386	8.703
11053	hsa-miR-32	-0.751	-1.682	9.228
28737	hsa-miR-106a	-0.410	-1.329	10.385
11048	hsa-miR-30a	-0.302	-1.232	11.382
4700	hsa-miR-140-5p	-0.574	-1.489	9.426

p-value	FDR adjusted p-value
2.54E-32	2.05E-29
3.54E-25	1.43E-22
1.54E-22	4.14E-20
3.29E-20	6.64E-18
1.33E-19	2.14E-17
3.45E-19	4.64E-17
2.39E-18	2.75E-16
2.18E-17	2.19E-15
1.30E-15	1.17E-13
7.04E-14	5.67E-12
8.89E-14	6.51E-12
2.00E-13	1.35E-11
4.33E-13	2.68E-11
2.39E-12	1.38E-10
4.15E-12	2.09E-10
5.63E-12	2.67E-10
6.81E-12	3.05E-10
1.30E-11	5.53E-10
3.53E-11	1.42E-09
1.41E-09	4.94E-08
3.03E-08	8.72E-07
1.72E-07	4.47E-06
1.69E-07	4.47E-06
2.97E-07	7.03E-06
5.34E-07	1.20E-05
5.52E-07	1.20E-05
5.93E-07	1.26E-05
9.26E-07	1.87E-05
2.26E-06	4.45E-05
3.63E-06	6.80E-05
7.79E-06	1.43E-04
8.90E-06	1.59E-04
1.06E-05	1.85E-04
2.21E-05	3.79E-04
2.43E-05	4.07E-04
2.90E-05	4.58E-04
2.90E-05	4.58E-04
3.74E-05	5.80E-04
6.89E-05	1.05E-03
8.88E-05	1.32E-03
1.11E-04	1.60E-03
1.54E-04	2.16E-03
2.04E-04	2.79E-03
5.12E-04	6.65E-03
5.78E-04	7.40E-03
1.13E-03	1.43E-02
1.50E-03	1.85E-02
2.71E-03	3.12E-02
4.13E-03	4.69E-02

MicroRNA	Target ID	Refs
miR-17	RUNX1	1,10
miR-17	NCOA3	1,2
miR-17	PCAF	1
miR-17	TGFBR2	1
miR-17	BCL2L11	1
miR-17	CCND1	1,10
miR-17	CDKN1A	1,3
miR-20a	PCAF	1
miR-20a	RUNX1	1,10
miR-20a	TGFBR2	1,9
miR-20a	E2F1	6,8
miR-20a	CCND1	10
miR-18a	CTGF	1
miR-19a	PTEN	1,5
miR-19a	THBS1	1
miR-19a	SOCS-1	7
miR-19b	SOCS-1	7
miR-92a	MYLIP	4
miR-92a	HIPK3	4

75x94mm (600 x 600 DPI)